



# A non-uniform grid approach for scheduling considering electricity load tracking and future load prediction

Giancarlo Dalle Ave<sup>a,b</sup>, Iiro Harjunkoski<sup>a,\*</sup>, Sebastian Engell<sup>b</sup>

<sup>a</sup>ABB Corporate Research Center Germany Wallstadter Str. 59, Ladenburg 68526, Germany

<sup>b</sup>Process Dynamics and Operations Group, Department of Biochemical and Chemical Engineering, Technische Universität Dortmund, Emil-Figge-Str. 70, Dortmund 44221, Germany

## ARTICLE INFO

### Article history:

Received 7 January 2019

Revised 18 June 2019

Accepted 30 June 2019

Available online 4 July 2019

### Keywords:

Resource-task network (RTN)

Demand side management

Intraday market

Day-ahead market

Discrete-time

Non-uniform grid

## ABSTRACT

Large consumers' electricity bills depend on many factors including: different electricity purchasing contracts and markets, deviation penalties, and grid fees. Two key markets are the intraday and the day-ahead markets. On the day-ahead market, the consumer commits to an amount of electricity that stacks upon their longer-term contract commitments. The next day, the consumer must follow this total demand profile to avoid paying deviation penalties. This total committed demand curve can be modified within the current day on the intraday market. In this work, a novel demand side management formulation is proposed that looks at a two-day scheduling horizon considering both the intraday and the day-ahead markets. As a result, instead of modeling a single-day load tracking problem a two-day problem is considered looking at both load following and future load prediction. Furthermore, the computational complexity of the problem is reduced with a non-uniform grid-based formulation. Results show that the novel formulation is able to effectively combine the intraday and day-ahead market concerns resulting in more realistic demand profiles than current formulations. Additionally, the non-uniform grid-based approach captures the key aspects of the formulation with a much lower computation time than the full-space approach.

© 2019 The Authors. Published by Elsevier Ltd.

This is an open access article under the CC BY-NC-ND license.

(<http://creativecommons.org/licenses/by-nc-nd/4.0/>)

## 1. Introduction

The increase of renewable energy generation from wind and solar, and the shift away from more traditional base-supply power systems presents a fundamental challenge to the world's power grid systems. Germany for example, is on target to reach a share of at least 25–35% of its electricity production from renewables by 2030, with a goal of 80% set for 2050 (Paulus and Borggrefe, 2011). Furthermore, it is estimated that given the appropriate technology, energy production from renewables is considered to be almost enough to cover all electricity consumption (Henriques and Stikkelman, 2017). This shift towards renewable energy thus presents a challenge to the electricity grid operator whose goal is to reliably match electricity supply and demand at any given moment. This is because renewable energy supplies are generally unresponsive to system needs and are associated with high levels of uncertainty. In

Germany it is estimated that the demand for positive and negative balancing power will increase by 33% and 41% respectively by 2030 (Paulus and Borggrefe, 2011). Therefore, stability and flexibility to the power system needs to be provided in different ways.

One method of providing this is through Demand Side Management (DSM). DSM refers to different ways of shaping the energy demand curve at the consumers' side. This benefits the electricity supplier through flattened load curves (thereby reducing required peak generation capacity) as well as enabling quick reaction to supply-demand mismatch in the grid by adjusting loads. While electricity consumers normally do not have any interest in tracking if there is a peak in electricity demand, there exist various programs to motivate them to reduce consumption at peak times. These programs can be classified into two types. The first first type is incentive-based programs whereby the utility or grid operators pay electricity consumers in order to get direct control on their non-crucial loads (Merkert et al., 2015). The second are price-based programs where the price of electricity changes throughout the day. These price-based programs are managed via contracts and markets and occur on various time scales. Generally speaking, the

\* Corresponding author.

E-mail addresses: [giancarlo.ave@de.abb.com](mailto:giancarlo.ave@de.abb.com) (G. Dalle Ave), [iiro.harjunkoski@de.abb.com](mailto:iiro.harjunkoski@de.abb.com) (I. Harjunkoski).

long-term contracts provide a baseload, which is agreed upon directly between large consumers and suppliers for terms of up to a year. Baseload contracts have a fixed electricity cost and represent loads which should always be met. Time-of-use (TOU) contracts are also often directly agreed upon between consumers and suppliers for periods of a few months. These contracts have multi-tiered prices for on- and off-peak times (e.g. day/night) and are often more expensive than baseload contracts. The advantage of TOU load contracts over baseload contracts is that the penalties associated with deviating from the contracted loads are not as steep (Erbach, 2016).

For shorter time periods, electricity is bought and sold on various markets. On the day-ahead market, consumers can purchase electricity loads typically at hourly amounts and prices, generally up to 12 h in advance of the first delivery for the next day. Note that while this is a market, if the bid of a customer is accepted the final price that is paid is the market clearing price. Thus, large consumers generally tend to bid conservatively in order to ensure that their bid is accepted and that they receive the amount of electricity that they need (Fleten and Kristoffersen, 2007). The total load that a consumer purchases from the aforementioned contracts and markets represents the total hourly committed load curve that a consumer must follow for the next day (24 h), within a tolerance (denoted the “penalty free” zone) or else so-called deviation “penalties” must be paid. The magnitude of the penalties is determined by the quick-acting balancing market. The balancing market ensures that the grid is balanced over a given interval and the price of electricity that is required to balance the grid is paid. In times of large demand shortages it is possible for electricity to be negatively priced, however this is an extreme case and normally a balancing cost is incurred for deviations. Thus, from a consumer's perspective, it is sufficient to treat deviations as a penalty paid.

In the event that a consumer experiences a major shift in their electricity demand (for example, in the event of a unit-breakdown) there also exists an intraday market in which consumers can modify their committed loads to avoid paying deviation penalties. Loads can be purchased on this market or existing committed loads can be sold. The volume traded on the intraday market is much smaller than that traded on the day-ahead market (EPEX, 2017). Furthermore, the intraday market often operates via a direct trading scheme where offers can be placed by both consumers or suppliers and directly accepted by another party. Taking these factors into consideration means that trading on the intraday market is much more constrained and expensive than trading on the day-ahead market and customers generally do not rely on it to completely meet their electricity requirements. To dissuade large production peaks, which can result in grid capacity problems, or to incentivize consumers shifting all their production to cheaper times there also exists critical peak pricing, where consumption peaks are billed with an additional fee. Consumption peaks in this case are capacity tariffs, where the maximum energy withdrawal at a single time point is penalized (European Distribution System Operators for Smart Grids, 2015). It has been shown that DSM from large-scale industrial processes could provide approximately 50% of capacity reserves for positive load balancing in 2020 (Paulus and Borggrefe, 2011). Furthermore, it is estimated that the economic benefit of DSM for European countries is in the billions of Euros, by providing savings in the areas of capital costs (from investments in generation and transmission) and operating costs (by enabling higher utilization of renewables) (Papadaskalopoulos et al., 2018). A diagram summarizing the various types of electricity contracts and markets can be seen in Fig. 1.

Due to the strong time-dependence of these electricity-related concerns, effective scheduling is essential in DSM, especially when a complex manufacturing process is involved (Zhang and Gross-

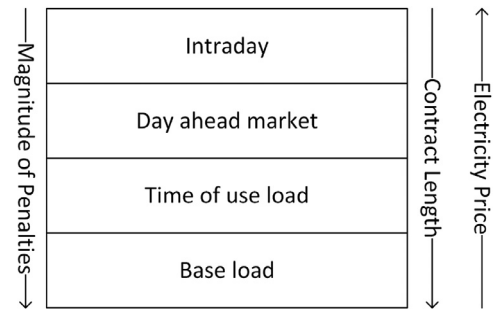


Fig. 1. A diagram of electricity contracts by length and price. The arrow points in the direction of increase.

mann, 2016). The area of scheduling is well established and a large number of studies have emerged using both continuous- and discrete-time approaches (Méndez et al., 2006). In recent years, scheduling under various energy constraints and electricity scenarios have gained increasing attention as it has been recognized as one of the challenges in industrial deployment of scheduling solutions (Harjunoski, 2016). Also in this direction, Zhang and Grossmann (2016) have noted the complex structure of electricity markets and indicate that more detailed modeling of market mechanisms is needed for DSM to continue to progress. As a result, many different studies have looked at different aspects of DSM applied to a wide variety of industries. One such industry is the cement industry where (Castro et al., 2009) developed both a continuous- and a discrete-time formulation for scheduling considering time-of-use prices with three different pricing levels. Another example can be found in (Basán et al., 2018) who studied air separation under a single time-varying price curve from the day-ahead market. Power-intensive continuous plants were also studied by Leo and Engell (2018a) and Leo and Engell (2018b) who used a two-stage stochastic programming approach to purchasing a load on the day-ahead electricity market. The first-stage decision regarding the quantity of electricity purchased on the day-ahead market needs to be tracked in the second-stage considering a combination of uncertain times of unit availability/breakdown, uncertain prices for deviating from the pre-purchased load, and uncertain product demands. An overview of industrial applications of DSM can be found in (Shoreh et al., 2016).

Steel plant scheduling, widely recognized as one of the most difficult industrial scheduling problems, has also been widely studied, even in the context of DSM. Ashok (2006) used a discrete-time model to minimize the operating cost of a mini steel plant. The operating costs include the price of power consumption under varying tariffs and a charge for the registered maximum demand. A continuous-time precedence model was proposed by Nolde and Morari (2010) for scheduling of stainless-steel making or tracking of a one-day contracted load under time-varying prices. Continuing in this direction Hadera et al. (2015) also proposed a continuous-time model precedence model for one-day multi-contract load tracking under time-varying pricing. A benefit to this model is that it is able to capture consumption over a given interval using fewer binary variables than its predecessor in (Nolde and Morari, 2010). More recently, Xu et al. (2018) proposed a new continuous-time event-based mixed-integer non-linear program (MINLP) model for steel making using an oxygen-furnace which, in addition to TOU energy prices, also considers the batching decisions. Zhao et al. (2018) looked at the scheduling of the rolling sector of a steel plant under time varying electricity prices. They also formulate the problem as an MINLP derived from generalized disjunctive programming (GDP) constraints, which they then reformulate as an mixed-integer linear program (MILP) to solve. Castro et al. (2013) also studied the load commitment problem for

melt shop optimization using a discrete-time Resource-Task Network (RTN) representation. The RTN formulation (Pantelides, 1994) is interesting as in its base form it is a generic modeling framework that can be readily extended to problem-specific features. Further in this direction, Zhang et al. (2017) also looked at using a discrete-time RTN for meltshop scheduling considering time-varying prices. This work considered flexible operation of the electric arc furnace in order to adapt its electricity consumption.

Due to the complicated manufacturing processes that are often involved, additional solution algorithms or decomposition approaches are often needed to solve scheduling problems in industrially relevant time-frames. One of the earliest endeavours in this area for steel production was by Harjunkski and Grossmann (2001), who split the problem of steel meltshop scheduling into five sub-problems each of which could be solved much faster than a full-space approach. Biondi et al. (2017) coupled production with maintenance scheduling for a melt-shop. To solve the resulting discrete-time model they utilize a non-uniform time grid approach. In regards to scheduling solution algorithms for DSM models Hadera et al. (2015) proposed a bi-level decomposition approach in which the reduced upper-level problem is used to fix binaries in the full-space lower level problem which in turns generates cuts for the upper-level problem. Xu et al. (2018) solve their MINLP model using a three-phase MILP-NLP decomposition strategy coupled with an enhanced spatial branch-and-bound algorithm. The use of rolling horizon algorithms has also been used for DSM scheduling models as in (Castro et al., 2013). The algorithm uses a combined discrete- and continuous-time approach to compute the schedule for a power intensive single stage multi-product plant. The aggregate model is a discrete-time model with a non-uniform grid which is used to calculate the number of event points for the detailed continuous-time portion of the model.

This work also looks at the problem of steel melt shop scheduling in a multi-contract electricity scenario but combines the interaction between the intraday and the day-ahead markets into a single problem. In order to do this, a two-day problem is solved. The first day considers a load commitment problem, whereby a pre-contracted load is tracked to within a tolerance or else deviation penalties are paid. It is possible to change this load only through transactions on the intraday market. The second-day problem involves a prediction of future consumption, to identify how much electricity should be bought, and at which times, on the day-ahead market in order to minimize future electricity and penalty costs. This contrasts current single-day approaches, which unrealistically model the two markets by considering them both to be active at the same time, or by ignoring one of the markets. Such two-day problems have been looked at from the point of view of an electricity supplier (De Ridder and Claessens, 2014), however, the production constraints associated with a larger consumer are much more complicated than from a producers point of view. As a result, this work is the first work to consider both markets in a single scheduling formulation from the point of view of a large electricity consumer.

Another benefit to using a two-day approach for large consumers is that it avoids a drop-off in production towards the end of the day. This differs from single-day formulations, which see a drop in production towards the end of the day as the considered jobs are completed. This is unrealistic as production is mostly performed on a continuous basis and is one of the factors hindering the application of DSM in industrial settings. The two-day problem rectifies this as jobs are allowed to start in one day and finish in the next, however they must be constrained to interact with the respective markets appropriately. In addition, this work also considers penalties paid on the maximum electricity consumption to avoid overly large peaks. The problem is formulated as a discrete-time RTN, and a non-uniform time grid approach is utilized to deal

with the size of the resulting two-day model. The remainder of the paper will discuss the problem features in detail (Section 2), followed by the formulation of the full-space discrete-time model (Section 3). Please note that a summarized version of Section 3 has previously been published in the proceedings of the Process Systems Engineering 2018 conference (Dalle Ave et al., 2018). This work expands on the details of this earlier work and further extends the work to the non-uniform grid-approach, the necessary model modifications and details of which will be discussed in Section 3.4. Numerical results comparing the current state of the art, the novel full-space model, and the rolling-horizon algorithm will be presented in Section 4. Lastly, conclusions and recommendations for further work will be discussed in Section 5.

## 2. Problem description

The first step in steel production is the melt shop where solid metal scrap is melted, endowed with its steel characteristics, and cast into slabs. Products are characterized by the grade of steel, width, and thickness of the slab. The process under consideration consists of four consecutive stages. The first stage is the electric arc furnace (EAF), which melts a batch (also known as a heat) of metal scrap by passing large amounts of electricity through the furnace's electrodes. From there the heat is transported to the Argon Oxygen Decarburizer (AOD) where an argon-oxygen mixture is injected into the melt in order to reduce its carbon content, forming steel. Following the AOD, a heat is processed by a Ladle Furnace (LF) where the chemistry and temperature of the heat are further adjusted. Lastly, the heat is processed in a continuous caster (CC) to form slabs of steel. In a melt shop the first three stages are operated in batch mode whereas the continuous caster is operated continuously. As a result, critical constraints apply to the continuous caster regarding the sequence and timing of batches arriving at the caster to ensure a continuous operation. A sequence of heats to be processed together in the CC is known as a heat group. A CC cannot process two heat groups back to back but requires a set-up time in between the two. In this work, two parallel identical machines are considered for the first three stages of production, while two parallel unique continuous casters are considered. The underlying RTN formulation however, is flexible and can readily be adapted to non-identical units at all stages (Castro et al., 2013). Between each of the stages, a heat is transported with some minimum and maximum time requirements. A block diagram of the process can be viewed in Fig. 2.

The aforementioned process consumes large amounts of electricity, a demand which must always be met. In this work, a detailed electricity market model is proposed that captures many of the electricity market details outlined in Section 1. A diagram summarizing the total committed electricity load for a plant, and the corresponding markets on which these loads can be traded can be seen in Fig. 3.

The problem addressed in this work can thus be summarized as follows: given the details of a plant's long-term contracts, as well as the total electricity load to be followed for the next 24 h (determined previously on the day-ahead market); determine the best production regime to track the current-day committed load while simultaneously predicting the amount of electricity to buy on the day-ahead market, and the corresponding production plan at that time. The goal of this is two-fold, on the one hand additional flexibility can be exploited by considering a two-day horizon for the electricity prices, and a more realistic production schedule can be achieved which allows jobs to start in one day and finish in the next. This formulation assumes that a good prediction of the prices of the day-ahead market exists, and that the price of deviations is known. These are reasonable assumptions as there exists a large number of electricity price forecasting techniques, on many

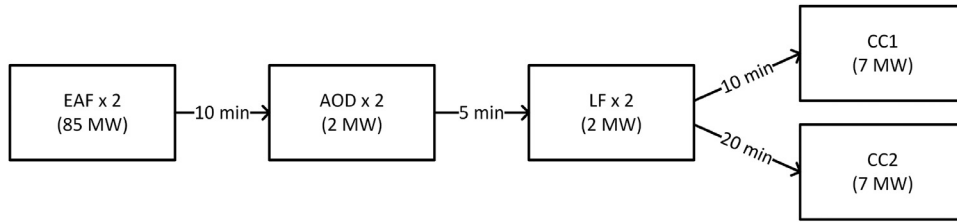


**Fig. 2.** A block flow diagram of the meltshop considered in this work. Unit electricity consumption is shown in brackets and minimum transportation times on the arrows between stages.

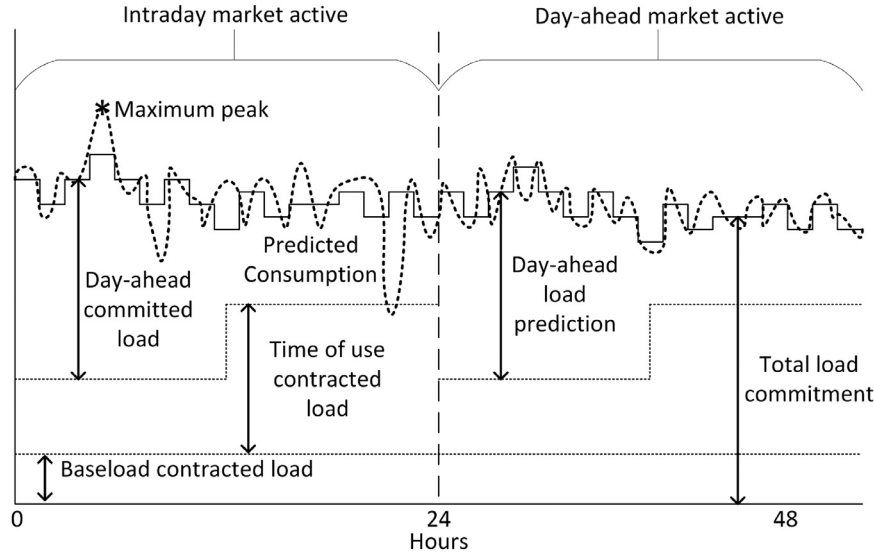


**Fig. 3.** Consumer's total electricity load commitment (solid line), consumption (dashed line), and the corresponding modification markets considered in this work.

different time-scales (Weron, 2014). Furthermore, since the intraday and day-ahead trading scheme are operated as markets, it is assumed that all bids are accepted at these aforementioned prices. The problem is formulated as a discrete-time RTN (Pantelides, 1994) and is applied to the problem of steel melt-shop scheduling.

### 3. Model description

The proposed model describes a power intensive steel making process with DSM considerations as described in Section 2. In this work, a discrete-time RTN model (Pantelides, 1994) is used to describe the problem. The RTN was chosen as it is generic and treats all resources in a uniform manner. In addition, it has been shown to be able to handle problems of industrial relevance (Wassick and Ferrio, 2011), and to be able to account for DSM (Castro et al., 2013). An RTN graphical description of the process can be viewed in Fig. 4 adapted from Castro et al. (2013). As previously mentioned, this work considers identical equipment for the first three production stages, which can therefore be aggregated together as a single resource at each stage. In order to model the transportation tasks it is necessary to split the location of a heat between stages into the heat exiting from one location and entering the subsequent location. This location could be machine specific (as in the case of the unique continuous casters) or the inlet to all the machines at a stage (in the case of identical, aggregated equipment).

A discrete-time model is used as the location of every time point in the grid is known in advance, allowing for straightforward modeling of intermediate events (such as changes in electricity pricing or power availability). In discrete-time formulations the scheduling horizon is divided into  $t \in T$  slots of size  $\delta$  minutes. The parameter  $\delta$  is chosen by the modeller to balance computa-

tional performance and model accuracy. The duration of a task ( $\tau$ ) in time slots is rounded-up to a multiple of  $\delta$ .

The remainder of this section will be used to describe the model parameters, variables and equations. In Section 3.1 the base formulation of the RTN model will be given. Sections 3.2 and 3.3 will go over the modeling extensions needed to model the steel-specific and DSM-specific constraints respectively. Lastly, Section 3.4 will detail the model expansions necessary to accommodate the non-uniform time grid. While the parameters and variables will be introduced throughout the text, a summary table of the terms can be viewed in Table A1 in Appendix A.

#### 3.1. Base RTN model

The RTN formulation represents the entire scheduling model as a set of resources ( $R$ ) and tasks ( $I$ ). In this formulation, tasks consume and produce sets of resources. Examples of resources include raw materials, final products, processing units, and electricity. Due to the nature of this problem, this formulation only considers a subset of the variables and parameters associated with the base RTN formulation. This is because heats in steel production are discrete entities, thus it is sufficient to only consider the binary extent variable  $N_{i,t}$ , which assigns the start of a task  $i \in I$  to time point  $t \in T$ .

Resources are managed through the non-negative continuous variable  $R_{r,t}$ , which represent the excess value of a resource  $r \in R$  at time  $t \in T$ . The key equation in the RTN formulation is the resource balance. The resource balance manages resource availability over the time grid by manipulating the amount of excess resources available at any given point and can be viewed in Eq. (1). The variable  $\Pi_{r,el,t}$  in this case, only applies to the electricity resource in order to track the consumption over time and to ensure that en-



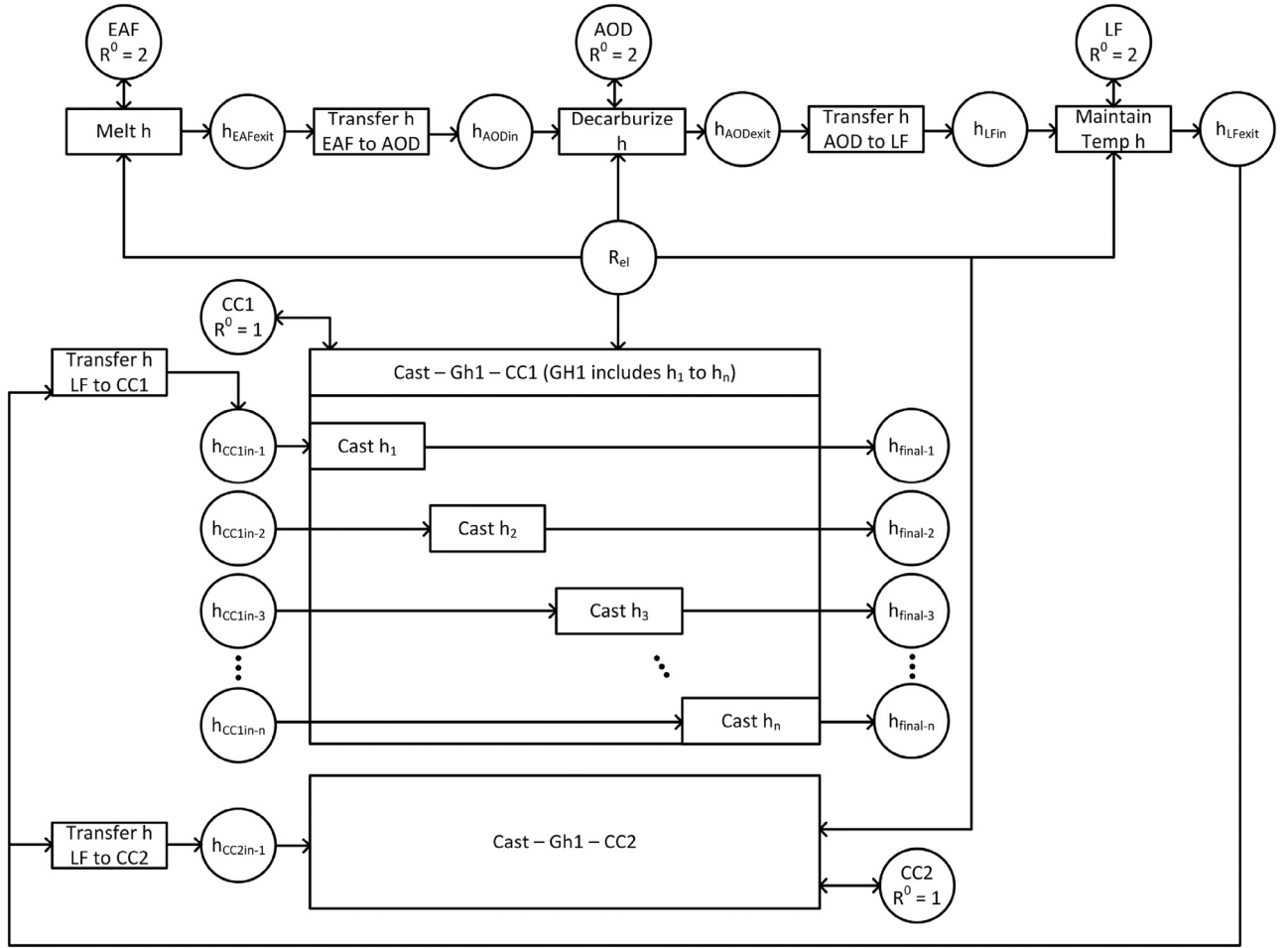


Fig. 4. The RTN diagram for the considered problem.

ergy does not propagate over time. The term  $R_{r,t-1}$  does not apply to the electricity balance for this same reason. The electricity resource balance will be explained in more detail later.

$$R_{r,t} = R_{r,t=1}^0 + R_{r \neq r^{el}, t-1 | t > 1} + \sum_{i \in I} \sum_{\theta=0}^{\tau_i} \mu_{r,i,\theta} N_{i,t-\theta} + \Pi_{r^{el},t} \quad \forall r \in R, t \in T \quad (1)$$

The only other equation that is necessary in the base RTN when considering only the binary extent of a task are capacity constraints on the excess resources. The capacity constraint is an upper bound on the availability of any given resource.

### 3.2. Steel plant model extension

In order to expand the RTN to model a steel meltshop environment additional constraints are needed. The meltshop specific constraints were first proposed in [Castro et al. \(2013\)](#). For completeness sake the constraints will be presented here but not discussed in great detail.

In order to ensure that a heat ( $h \in H$ ) is executed in one unit ( $u \in U$ ) at each stage ( $k \in K$ ) and that each group of heats ( $g \in G$ ) is processed in the caster once, [Eqs. \(2\) and \(3\)](#) are used. Note that the set  $I_{h,u}$  indicates tasks that can process heat  $h$  on unit  $u$ .

$$\sum_{u \in U_k} \sum_{i \in I_{h,u}} N_{i,t} = 1 \quad \forall h \in H, k = 1, 2, 3 \quad (2)$$

$$\sum_{u \in U_k} \sum_{i \in I_{g,u}} N_{i,t} = 1 \quad \forall g \in G, k = 4 \quad (3)$$

The same logic applies to transfer tasks. [Eq. \(4\)](#) ensures that each transfer task is executed once while [Eq. \(5\)](#) approximates the maximum transfer time of a heat by placing restrictions on the lifetime of its intermediate resource based on the max and min transfer time between the stages ( $maxtrf_{u,u'}$  and  $mintrf_{u,u'}$  respectively).

$$\sum_{u \in U_k} \sum_{u' \in U_{k+1}} \sum_{i \in I_{h,u,u'}} N_{i,t} = 1 \quad \forall h \in H, k \neq 4 \quad (4)$$

$$\sum_{r \in R_{h,u}^{el}} \sum_{t \in T} R_{r,t} \leq \left\lceil \max_{\substack{u \in U_k \\ u' \in U_{k+1}}} (maxtrf_{u,u'} - mintrf_{u,u'}) / \delta \right\rceil \quad \forall h \in H, k \neq 4 \quad (5)$$

To complete the approximation of maximum transfer time, the resource availability for all heats at the exit location of a stage are constraints to be zero. This forces the transportation task for a heat between two consecutive stages to be executed immediately after a heat is produced, thereby accounting for the minimum transportation time between the stages. Therefore, only the steel heats at the input location to a stage are allowed to exist for multiple time periods. Thus, [Eq. \(5\)](#) ensures that they do not exist for longer than the maximum time they are allowed to wait between consecutive stages. The excess amount of electricity is also constrained to be zero. This is to prevent build-up of electricity as well as to ensure that the external variable  $\Pi_{r^{el},t}$ , which will be used to link the production and DSM models, correctly tracks the consumption of electricity over time. An upper limit on the maximum power

consumption is defined in Eq. (6).

$$\Pi_{rel,t} \leq \sum_{u \in U} \left( \max_{h \in H} (power_{h,u}) \right) \quad \forall t \in T \quad (6)$$

### 3.3. DSM model extension

Now that the power consumption over time can be tracked, it is possible to link it with the constraints necessary to model how the different electricity markets and contracts function. In order to calculate the deviations from the hourly ( $T_{hr}$ ) load committed to for the first day ( $y_{t \in T_{hr}}^{CL}$ ), two equations are needed. Note that the notation  $t \in T_{hr}$  in the committed load parameter refers to the fact that the committed load is constant for all time points within a given hour. The first equation, is used to account for the time before it is possible to trade on the intraday market ( $T_{sell}$ ). It is necessary to account for this time as it varies greatly between countries. For example, in Germany, electricity can be traded on the intraday market up to half an hour before the time of delivery. However, in Italy the intraday market takes the form of five separate auctions throughout the day, so it is possible to have to wait several hours until it is possible to modify the previously committed electricity profile. The deviations in this case can be tracked using three variables. The first one is the continuous variable  $\Delta_t$ , which represents the deviation from the previously purchased day-ahead load. The second is the free variable  $\omega_t$ , which represents the penalty free region. Only these variables are needed to track the deviations before the next possible trading period on the intraday market ( $T_{sell}$ ). After trading on the intraday market is possible, an additional continuous variable  $\sigma_t$  is needed. This represents the load change of the committed load on the intraday market. The set  $T_{intra}$  is used to define the length of intervals which can be traded and match them to the underlying discrete-time grid. For example, in Germany, electricity can be traded in 15 min intervals on the intraday market, while in France it is traded in hourly blocks. The two equations to calculate the deviations paid before and after trading on the intraday market is possible can be seen in Eqs. (7) and (8) respectively.

The equations state that the total amount of electricity consumed in any given time period (within the first day), must be equal to the amount of electricity committed to in advance, plus the deviations ( $\Delta_t$ ), including the penalty free region ( $\omega_t$ ), and the amount of electricity bought or sold from the intraday market ( $\sigma_t$ ). Lastly, Eq. (9) is used to ensure that all time points within an intraday trading interval are the same. This is necessary because the electricity and deviations need to be tracked at every  $t \in T$ , but energy may be traded on the intraday market in intervals larger than  $\delta_t$ . Therefore, a constraint is needed to ensure that the amount of electricity sold at each interval within  $T_{intra}$  (i.e.  $t \in T_{intra}$ ) is the same. Therefore this constraint dictates that all discrete-time intervals within a given period of trading are consistent with one another in regards to the amount traded. Please see Fig. 5 for a graphical explanation.

In regards to the set notation used, note that  $T_{intra}$  is a subset of  $T$  and denotes the set of time periods which correspond to a single interval in which electricity can be bought or sold on the intraday market. The notation  $T_{intra} \in T_{day1}$  therefore refers to all such intervals within the first day of the scheduling horizon ( $T_{day1}$ ). This notation will be used throughout the paper to denote time points within a given subset of the time horizon, and all subsets within the time horizon. This is also illustrated in Fig. 5.

$$\Pi_{rel,t} = y_{t \in T_{hr}}^{CL} + \omega_t + \Delta_t \quad \forall t \in T_{day1} < T_{sell} \quad (7)$$

$$\Pi_{rel,t} = y_{t \in T_{hr}}^{CL} + \omega_t + \Delta_t + \sigma_t \quad \forall t \in T_{day1}, t > T_{sell} \quad (8)$$

$$\sigma_t = \sigma_{t'} \quad \forall t, t' \in T_{intra}, t \neq t', T_{intra} \in T_{day1} \quad (9)$$

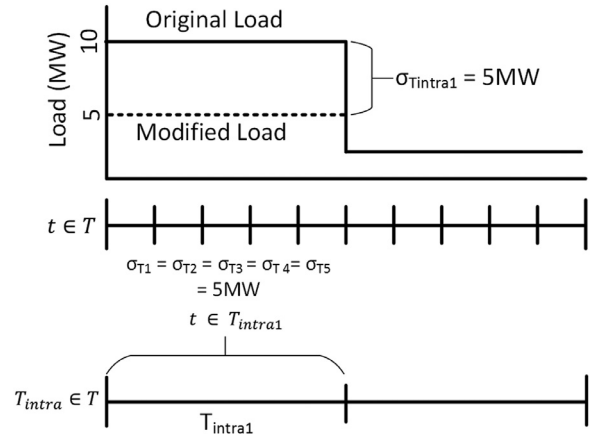


Fig. 5. A diagram of the relation between the intraday timeslots and the discrete-time grid time slots.

In order to account for deviations from different contracts the term ( $\Delta_t$ ) is then split according to Eq. (10). In this case the non-negative continuous variables  $\Delta_t^{DA}$ ,  $\Delta_t^{TOU}$ ,  $\Delta_t^{BL}$  represent negative deviations from the day-ahead, TOU, and baseload contracts respectively. It is necessary to separate the deviations from each of the contracts, because they are penalized differently. The magnitude of the penalties paid is generally determined by the balance-market, however, deviations from the TOU and baseload contracts are additionally penalized for breaking the terms of their respective contract. The longer the duration of the contract, the more expensive the penalty for violating the terms of the contract (e.g. deviations from the base load are more expensive than deviations from the TOU, which in turn are more expensive than deviations from the day-ahead committed loads). Therefore, an extra binary variable is not needed to account for which contract is being violated, as the optimal solution will first penalize the shorter contracts before proceeding to the longer ones. Going in the opposite direction  $\Delta_t^+$  represents positive deviations from the total contracted load, with the magnitude of the penalty being determined solely on the balance-market. A figure illustrating the different deviations, as well as some of the other parameters, can be viewed in Fig. 6.

$$\Delta_t = \Delta_t^+ - \Delta_t^{DA} - \Delta_t^{TOU} - \Delta_t^{BL} \quad \forall t \in T \quad (10)$$

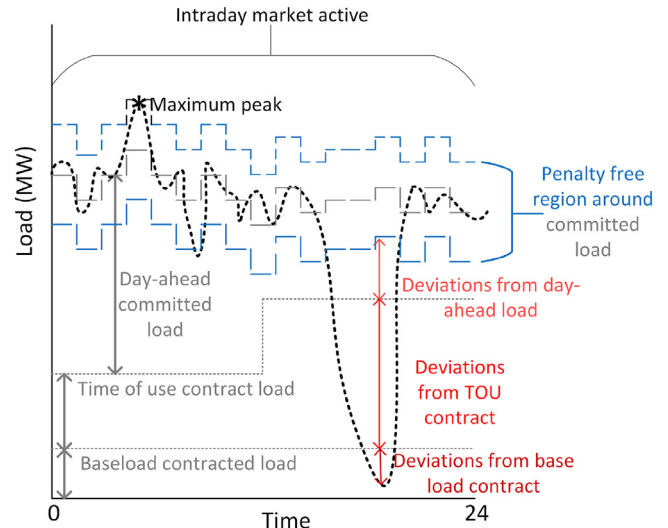


Fig. 6. A visualization of the deviations other electricity market-related concerns.

A similar disaggregation is also needed for the load change variable  $\sigma_t$ . The term is split to account for the load purchased from the intraday market ( $\sigma_t^+$ ), the load sold from the day-ahead contract ( $\sigma_t^{DA}$ ), the TOU contract ( $\sigma_t^{TOU}$ ), and the baseload contract ( $\sigma_t^{BL}$ ). It is necessary to split the term to ensure that the magnitudes of the penalty free region and the deviations can be enforced (more on this later). Similar to the deviations it is not necessary to use an additional variable to track which contract is being sold from as electricity is cheaper from the longer term contracts. Therefore, in general, the optimal solution will first sell electricity from the shorter contracts before selling electricity from the longer ones. Note that depending on the projected price of electricity on the intraday market, it is also possible to make a larger profit from selling electricity from the longer term contracts. By disaggregating the variables it is possible to account for situations such as this. This disaggregation can be seen in Eq. (11). In a similar manner to Eq. (9) the set of equations described in Eq. (12) are used to ensure that the amount traded from each contract remains constant over an intraday trading interval. Since the intraday market is much smaller than the day-ahead market, upper bounds are also placed on the these load change amounts. In general, this amount is highly dependent on market conditions, as well as the terms of each of the contracts, and would need to be set by an experienced energy trader.

$$\sigma_t = \sigma_t^+ - \sigma_t^{DA} - \sigma_t^{TOU} - \sigma_t^{BL} \quad \forall t \in T \quad (11)$$

$$\begin{aligned} \sigma_t^+ &= \sigma_{t'}^+ & \forall t, t' \in T_{intra}, t \neq t', T_{intra} \in T_{day1} \\ \sigma_t^{DA} &= \sigma_{t'}^{DA} & \forall t, t' \in T_{intra}, t \neq t', T_{intra} \in T_{day1} \\ \sigma_t^{TOU} &= \sigma_{t'}^{TOU} & \forall t, t' \in T_{intra}, t \neq t', T_{intra} \in T_{day1} \\ \sigma_t^{BL} &= \sigma_{t'}^{BL} & \forall t, t' \in T_{intra}, t \neq t', T_{intra} \in T_{day1} \end{aligned} \quad (12)$$

The amount of load to commit to on the day-ahead market for the second day is determined via Eq. (13). The equation is very similar to Eq. (7), however instead of being a parameter, the load to commit to is a non-negative continuous variable ( $y_t^{PL}$ ). This represents the total electricity commitment for the second day, thus giving the amount of electricity to buy from the day-ahead market. The goal is to set the load in the future such that the minimum amount of deviations are paid and to take advantage of time-dependent electricity prices by producing more when it is cheaper to do so. In order to enforce that only a single load is purchased per hour, Eq. (14) is used.

$$\Pi_{rel,t} = y_t^{PL} + \omega_t + \Delta_t \quad \forall t \notin T_{day1} \quad (13)$$

$$y_t^{PL} = y_{t'}^{PL} \quad \forall t, t' \in T_{hr}, t \neq t', T_{hr} \notin T_{day1} \quad (14)$$

Since the baseload and TOU contracts are longer-term, they generally represent loads that must always be met. As such, the penalty-free region is calculated without consideration of these longer-term contracted loads ( $y_{t \in T_{hr}}^{TOU}$  and  $y_{t \in T_{hr}}^{BL}$  for the TOU and baseload contracted loads respectively). Thus, the amount of electricity that comes from the day-ahead market can be determined using Eqs. (15) and (16). Again the notation  $t \in t_{hr}$  is used to indicate a parameter that is constant over an hourly interval. Conversely, the variable,  $y_t^{DA}$  is used to denote the day-ahead load, which is calculated based on the total predicted load for a specific time slot. Bounds on the predicted loads are then given in Eq. (17). The lower bound states that the predicted future load cannot be lower than the sum of the long-term contracted loads (as these long-term contracts cannot be modified on the day-ahead market). The upper bound is the max consumption of the plant.

$$y_t^{DA} = y_{t \in T_{hr}}^{CL} - y_{t \in T_{hr}}^{TOU} - y_{t \in T_{hr}}^{BL} \quad \forall t \in T_{hr}, T_{hr} \in T_{day1} \quad (15)$$

$$y_t^{DA} = y_t^{PL} - y_{t \in T_{hr}}^{TOU} - y_{t \in T_{hr}}^{BL} \quad \forall t \in T_{hr}, T_{hr} \notin T_{day1} \quad (16)$$

$$y_{t \in T_{hr}}^{TOU} + y_{t \in T_{hr}}^{BL} \leq y_t^{PL} \leq \sum_{u \in U} (\max(\text{power}_{h,u})) \quad \forall t \notin T_{day1} \quad (17)$$

The penalty-free region is then calculated as a percentage ( $c_{pf}$ ) of the day-ahead committed load (defined above) taking into account what has been traded on the intraday market. The upper and lower bounds on the penalty free region for the current-day and for the future load prediction can be viewed in Eqs. (18) and (19) respectively.

$$-c_{pf}^{DA} * (y_{t \in T_{hr}}^{DA} + \sigma_t) \leq \omega_t \leq c_{pf}^{DA} * (y_{t \in T_{hr}}^{DA} + \sigma_t) \quad \forall t \in T_{hr}, T_{hr} \in T_{day1} \quad (18)$$

$$-c_{pf}^{DA} * y_t^{DA} \leq \omega_t \leq c_{pf}^{DA} * y_t^{DA} \quad \forall t \in T_{hr}, T_{hr} \notin T_{day1} \quad (19)$$

If the actual consumption strays outside of the penalty-free region defined above, penalties must be paid. Eqs. (20)–(22) define the bounds on the deviations on the electricity purchased from the day-ahead market. Three equations are needed to bound the negative deviations, one to take into account the deviations before the next intraday trading period, where anything outside the penalty-free region is a deviation. Another to account for the time after it is possible to trade on the intraday market, where the load change due to intraday trading is considered. Lastly, the third is needed to account for the deviations based on the load prediction for the second day. Positive deviations are not directly capped, but it is possible to add a tightening constraint for the positive deviations similar to that in Eq. (6).

$$\Delta_t^{DA-} \leq (1 - c_{pf}^{DA}) * y_{t \in T_{hr}}^{DA} \quad \forall t < T_{sell} \in T_{hr}, T_{hr} \in T_{day1} \quad (20)$$

$$\Delta_t^{DA-} \leq (1 - c_{pf}^{DA}) * (y_{t \in T_{hr}}^{DA} + \sigma_t) \quad \forall t \geq T_{sell} \in T_{hr}, T_{hr} \in T_{day1} \quad (21)$$

$$\Delta_t^{DA-} \leq (1 - c_{pf}^{DA}) * y_t^{PL} \quad \forall t \in T_{hr}, T_{hr} \notin T_{day1} \quad (22)$$

Limits on the deviations from the TOU and base load contracts can be found in Eqs. (23) and (24) respectively. Deviations from these contracts are more costly as in addition to the amount paid due to the balancement markets an additional penalty is added by the supplier. Thus, they need to be tracked separately from the other deviations. As previously mentioned, it is not necessary to manually enforce the order between the different kinds of deviations as the deviations from the longer contracts are penalized more heavily than those from shorter contracts and thus the optimization process itself will naturally use the shorter-term deviations before progressing onto the others.

$$\Delta_t^{TOU-} \leq y_{hr}^{TOU} - \sigma_t^{TOU} \quad \forall t \in T \quad (23)$$

$$\Delta_t^{BL-} \leq y_{hr}^{BL} - \sigma_t^{BL} \quad \forall t \in T \quad (24)$$

Eq. (25) calculates the maximum peak at any given instance over the time horizon. Note that in this case the set  $T_{peak}$  indicates the fact that in some cases the peak is only measured during times of peak energy usage. Therefore, the peak only needs to be tracked over these specific intervals. To account for the fact that the peak may be penalized only once per billing period (e.g. once a week or once a month) Eq. (26) sets the peak to at least the maximum peak achieved to date ( $\xi_{toDate}$ ).

$$\xi \geq \Pi_{rel,t} \quad \forall t \in T_{peak} \cap T \quad (25)$$

$$\xi \geq \xi_{toDate} \quad (26)$$

To recap, the proposed formulation considers three different time grids. The first is the base discrete-time grid, based upon which the scheduling is done. Built on top of this are the grids representing the intervals over which electricity can be traded on the intraday market, or the intervals over which electricity is bought on the day-ahead market. These additional grids are matched to the underlying grid and the granularity of the discrete-time grid should be chosen with this in mind. Thus the notation  $t \in T_{intra}$  corresponds to the discrete-time intervals  $t$  matched to a specific

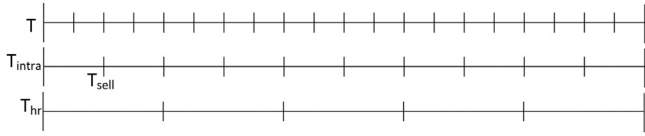


Fig. 7. An example of the various time grids and how they align.

interval  $T_{intra}$ . As previously mentioned, the notation  $T_{intra} \in T$  then denotes all such intervals within the given time horizon. A diagram of the various time grids can be viewed in Fig. 7. The flexibility that is provided by considering the multiple time-grids also allows for the resulting model to consider DSM scenarios which vary from market to market. For example, in Belgium trading on the intraday market is conducted in 5 min intervals, while in Germany it is traded over 15 min intervals. In this formulation, the size of the intraday trading intervals can be easily updated by changing the way the intraday trading grid matches up with the discrete time grid. Therefore, it is easy to account for different DSM situations as it is only a matter of updating this matching, instead of updating the model itself. In Section 4, two different DSM scenarios will be presented, highlighting the flexibility of this approach.

The objective function of the problem is to minimize the total electricity cost of production. This includes cost of the electricity from each of the contracts, the total cost of deviations, revenue or costs incurred by trading on the intraday market, and a flat fee paid on the maximum peak attained during production. Some auxiliary equations will be defined in Eqs. (27) and (28) in order to make the objective function easier to follow. These equations represent the actual amount of electricity consumed from the TOU and baseload contracts respectively ( $\Pi_{rel,t}^{TOU}$  and  $\Pi_{rel,t}^{BL}$ ), taking into account the amount sold from these contracts on the intraday market as well as the amounts deviated from them. The complete objective function can then be viewed in Eq. (29). The first line in the equation represents the total cost of electricity consumed from all contracts (where  $C_t$  denotes the cost of electricity at time  $t$  for each of the three considered contracts). The second line calculates the total cost of the deviations paid from each of the contracts. The third line sums up the amount of money traded on the intraday market. Note that this amount can be positive or negative depending on if a net value of electricity was bought or sold. Lastly a flat penalty is paid on the maximum peak consumption achieved.

$$\Pi_{rel,t}^{TOU} = y_t^{TOU} - \Delta t^{TOU} - \sigma_{t_{intra}}^{TOU} \quad (27)$$

$$\Pi_{rel,t}^{BL} = y_t^{BL} - \Delta t^{BL} - \sigma_{t_{intra}}^{BL} \quad (28)$$

$$\begin{aligned} \min \quad & \sum_{t \in T} (C_t^{DA} * (\Pi_{rel,t} - \Pi_{rel,t}^{TOU} - \Pi_{rel,t}^{BL}) + C_t^{TOU} \Pi_{rel,t}^{TOU} + C_t^{BL} \Pi_{rel,t}^{BL}) \\ & + \sum_{t \in T} (C_t^+ \Delta t^+ + C_t^{DA-} \Delta t^{DA-} + C_t^{TOU-} \Delta t^{TOU-} + C_t^{BL-} \Delta t^{BL-}) \\ & - \sum_{t_{intra} \in T} \sum_{t \in T_{intra}} (C_t^{DA_{sell}} \sigma_{t_{intra}}^{DA} + C_t^{TOU_{sell}} \sigma_{t_{intra}}^{TOU} + C_t^{BL_{sell}} \sigma_{t_{intra}}^{BL} - C_t^{buy} \sigma_{t_{intra}}^+) \\ & + C^{peak} \xi \end{aligned} \quad (29)$$

#### 3.4. Non-uniform time grid model

The downside to considering a two-day problem over two one-day problems is that the resulting two-day optimization problem is very large. To address this problem, a non-uniform time grid approach is presented along with its potential application in a rolling-horizon scheme. Multi-time scale methods have repeatedly demonstrated their capability to solve medium/long term scheduling problems of complex production systems since their introduction in (Papageorgiou and Pantelides, 1996). The main idea of these

methods is to reduce the complexity of the problem by directly addressing the different time horizons of the problem. Normally this is applied to planning and scheduling where the problem is broken down into two parts; the first ascertains the planning decisions, while the second takes care of the more detailed scheduling decisions. The following approach follows the same type of methodology but the less detailed “planning” portion of the model abstracts some of the detailed timing and electricity market constraints which are present in the full detailed scheduling portion of the model.

This formulation utilizes a non-uniform time grid. In the near future, the time intervals are of size  $\delta_{detail}$ . This model is henceforth known as the detailed model, consisting of time points  $T_{detail}$ . Further into the future, the time intervals are elongated to size  $\delta_{agg}$  (the aggregate model, with the set of time points  $T_{agg}$ ). The parameter  $\delta_{detail}$  should be chosen in a way that captures the finer aspects of the task and electricity market timings.  $\delta_{agg}$  on the other hand, should be chosen such that the size is great enough to reduce the complexity of the problem, while still capturing the major details of the scheduling and electricity market formulations. A diagram of the non-uniform grid timeline can be viewed in Fig. 8.

In order to account for the non-uniform time grid, several equations need to be modified. The first modification is the resource balance. Due to the non-uniform nature of the grid, the duration of a task in time slots will change over the length of the horizon. Thus, both the task duration parameter  $\tau$  and the discrete interaction parameter  $\mu$  need to be indexed by time ( $\tau_{i,t}$  and  $\mu_{r,i,t,\theta}$  respectively). The modified resource balance can be viewed below in Eq. (30). It is interesting to note that this is the same approach that is needed to expand the discrete-time RTN to consider preemptive tasks (Castro et al., 2018).

$$\begin{aligned} R_{r,t} = & R_{r|t=1}^0 + R_{r \neq rel,t-1} \\ & + \sum_{i \in I} \sum_{\theta=0}^{\tau_{i,t}-\theta} \mu_{r,i,t-\theta} N_{i,t-\theta} + \Pi_{rel,t} \quad \forall r \in R, t \in T \end{aligned} \quad (30)$$

When considering a larger time slot in the aggregate model, flexibility in the solution may be lost as a result of rounding up task duration to the nearest time slot. This is a problem of discrete-time approaches in general, however, the time discretization in the aggregate model is coarser than that of the detailed resulting in even more accuracy loss. This can potentially cause problems with the complex timing-related constraints, thus the maximum wait constraint needs to be updated to account for the larger interval sizes in the aggregate model to ensure feasibility over the scheduling horizon. The updated constraint can be viewed in Eq. (31).

$$\begin{aligned} & \sum_{r \in R_{h,u}^{ll}} \sum_{t \in T_{detail}} R_{r,t} \cdot \delta_{detail} + \sum_{r \in R_{h,u}^{ll}} \sum_{t \in T_{agg}} R_{r,t} \cdot \delta_{agg} \\ & \leq \max_{\substack{u \in U_k \\ u' \in U_{k+1}}} (maxtrf_{u,u'} - mintrf_{u,u'}) \quad \forall h \in H, k \neq 4 \end{aligned} \quad (31)$$

Another concern in the non-uniform model is the calculation of the maximum electricity peak. In order to account for the time difference over which the maximum peak is calculated, the peak calculation is separated into two parts. One part for the detailed ( $\xi_{detail}$ ), and one for the aggregate portion of the model ( $\xi_{agg}$ ). An example where this is necessary follows: an EAF task takes 90 min. The discretization is 15 min in the detailed model and 60 min in the aggregate. If, for example, two EAF tasks need to be scheduled within a three-hour interval, it is possible to position them in the detailed portion of the model such that they do not overlap. This is not true for the aggregate part of the model as the two tasks must overlap (due to the rounding of the task durations), thus creating a peak twice as large than what is actually necessary. This





Fig. 8. An example of the non-uniform grid timeline.

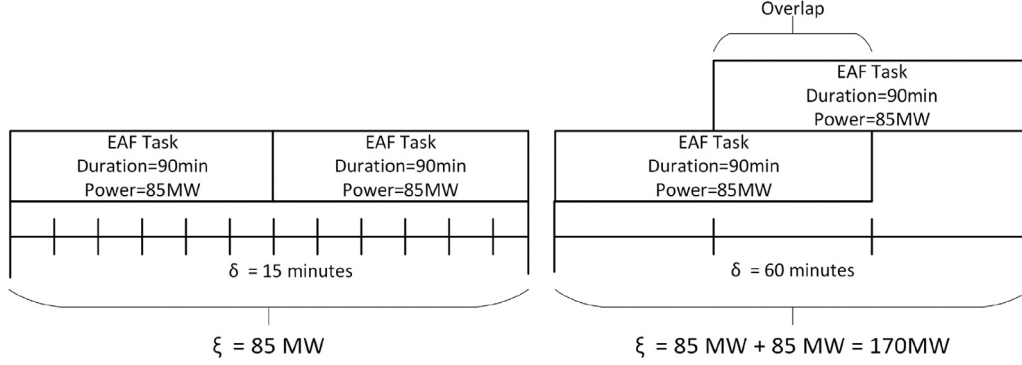


Fig. 9. A graphical illustration of why it is necessary to split the maximum peak calculation between the detailed and aggregate models.

example is visualized in Fig. 9. Therefore, it is important to separate the peaks between the different portions of the model and penalize them accordingly in the objective function. These updated constraints can be viewed in Eqs. (32) and (33). Similarly, the maximum overall consumption, considering the detailed, aggregate and the peak to date can be set using Eq. (34). Note that these peaks could be penalized in the objective function in combination with one another, or by considering only the overall maximum peak ( $\xi$ ). The corresponding terms would need to be added to the objective function described in Eq. (29).

$$\xi_{detail} \geq \Pi_t \quad \forall t \in T_{peak} \in T_{detail} \quad (32)$$

$$\xi_{agg} \geq \Pi_t \quad t \in T_{peak} \in T_{agg} \quad (33)$$

$$\begin{aligned} \xi &\geq \xi_{detail} \\ \xi &\geq \xi_{agg} \\ \xi &\geq \xi_{toDate} \end{aligned} \quad (34)$$

### 3.5. Rolling horizon scheme

This non-uniform time grid approach can readily be extended to a rolling/shrinking horizon scheme for online scheduling use. This can be accomplished by fixing a subset of the variables in the current detailed model and extending the length of the detailed model in the next iteration. This can be repeated until the whole schedule is calculated in detail. An example of such an approach can be seen in Fig. 10.

Going into more detail for this example, in the first iteration of the rolling horizon, the detailed model counts for one fourth of the total horizon. Once the optimization has been run for this subproblem it is possible to fix the variables of the current detailed model. In this case the entire length of the detailed model is fixed. The length of the detailed model can then be extended in the next iteration. In this example, in Iteration 2, the detailed model accounts for half of the total scheduling horizon. Note that the first half of the detailed model is fixed so the size of the unfixed detailed model in Iteration 2 is the same size as in Iteration 1. This ensures that each subproblem will have a lower computation time compared to the full-space model. This process can be repeated until the end of the fourth iteration when the entire horizon has been scheduled in detail. Note that it is also possible to fix only a subset of the detailed model (for example only the first half) at each iteration. The length of the detailed model in the subsequent iteration is then extended by the length of the duration that has been fixed. This ensures that the length of the unfixed detailed model stays the same at every iteration while allowing for more flexibility between iterations as a period overlaps between the two subproblems. A diagram of this can be seen in Fig. 11.

The benefits of the described approach is multifaceted. The first benefit is that a detailed schedule is quickly calculated for the immediate future providing a plan to execute going forward. Secondly, the planning decisions (e.g. load to commit to on the day-ahead market) need not be known immediately, and thus can be calculated in subsequent iterations of the rolling-horizon algorithm

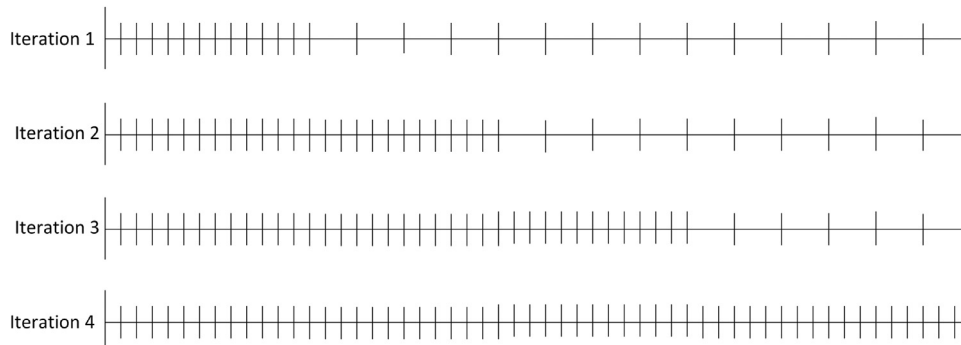


Fig. 10. An example of the non-uniform grid approach and its use in a rolling horizon algorithm.

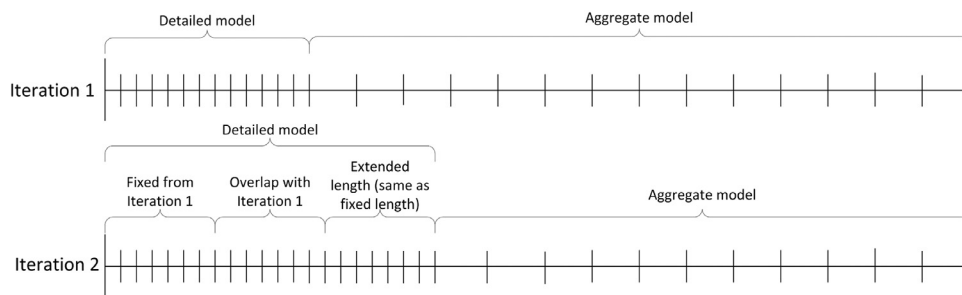


Fig. 11. An example of two subsequent iterations of the rolling horizon approach considering an overlap between the subproblems of the two iterations.

which can be performed “offline”. Lastly, the coarse aggregation of the aggregate model should provide the flexibility needed for later scheduling revisions, which is necessary for online scheduling approaches (Gupta et al., 2016). In fact, one complete execution of the rolling horizon approach represents the online approach assuming there are no disturbances over the scheduling horizon and calculating the next iteration after a set amount of time.

An example of how the approach could be used online follows. At the start of Day 1 (hour 0) the first iteration of the rolling horizon algorithm can be quickly computed, providing a detailed schedule for the first few hours of production while ensuring feasibility in the long-run. In the event of a disturbance, the schedule can be recomputed quickly for the upcoming hours in a shrinking horizon approach. During normal execution, the remainder of the rolling horizon algorithm can be run to determine the longer-term planning decisions. Before the day-ahead market closes (hour 12), final purchases can be made according to the long-term planning decisions. This load would then represent the committed load for hours 24–48. The horizon would continue to shrink until hour 24 when it is possible to do planning for the third day (hours 48–72). Numerical results of the algorithm behaving in a simulated online setting will be presented in Section 4.4.

#### 4. Results and discussion

This paper seeks to show illustrate multiple aspects. The first is a direct comparison between the current state of the art by comparing the solution of two one-day DSM problems with the solution of the proposed two-day problem. This comparison will be extended by implementing the non-uniform time grid approach. To facilitate a fair comparison, and to quantify the losses due to the non-uniform time grid approach, the aforementioned rolling horizon approach will be used to calculate in detail the entire horizon length. Secondly, the paper will analyse the difficulty in converging to a provably optimal solution and discuss the effect of computation time on solution quality. Furthermore, this work will investigate whether the predicted loads can be accurately followed by the algorithm. Then, the two-day approaches will be compared in an online setting, responding to a poor estimation of batch time as well as to the addition of a rush order. Lastly, the flexibility of the formulation will be shown by presenting the results from cases with different parameter sets. Parameters for the model, including batch duration and steel heat group matchings, can be found in Appendix B (Tables B1 and B2 respectively).

In regards to the electricity market models, the case studies consider that electricity can be bought in hourly intervals on the day-ahead market. The penalty of deviating from this day-ahead load is 150% of the day-ahead electricity cost. The penalty for under-consuming from the TOU or baseload contracts is 150€/MWh and 200€/MWh respectively. The TOU contract in this case has off- and on-peak pricing with corresponding loads of 10 and 5 MW respectively. The baseload is contracted for 5 MW.

While this may seem low, the meltshop area of a steel plant has a very variable electricity consumption (depending on how many EAFs are currently in use), thus it is generally not responsible for ensuring that the baseload contracted load is met. A table summarizing the pricing scheme and committed electricity loads can also be found in Appendix B (Table B3). The discretization of the RTN model is 15 min in this case. For the rolling horizon cases, the aggregate model is discretized to a granularity of 60 min. All the models in this work were formulated in GAMS 24.7.4 and solved using CPLEX 12.6.3.0.

##### 4.1. Comparison of current state-of-the-art and new formulation

To compare the different model scenarios three case studies will be used. Case 1 considers two one-day problems in which pre-determined loads must be followed with no consideration of the intraday market (i.e. no possibility to change said committed load) or of the maximum peak (i.e. the production peak is tracked for the sake of comparison, but not penalized in the objective function). This represents a worst-case scenario as in reality it would be possible to make some changes to the current committed load on the day ahead market. Case 2 is similar to Case 1 except the committed load is treated as a decision variable instead of a parameter. This means that within a given day, Case 2 has complete flexibility over its load and how to follow it. This is overly ideal as the markets do not allow for simultaneous load prediction and following. In reality the committed load for at least the first day would be fixed (as this load was purchased in advance on the day-ahead market), and only limited modifications would be allowed via the intraday market. Cases 1 and 2 therefore represent the current *status quo* for DSM modeling, which offers either an overly pessimistic (as in Case 1 where no flexibility is allowed), or an overly optimistic view of DSM (as in Case 2 where an unrealistic amount of flexibility is allowed). Additionally, peak management is also not considered in current works, which we will show is an important aspect of DSM.

Case 3 is the proposed full-space approach, which more realistically models the constraints of the electricity markets. This case highlights the importance of considering a longer horizon in order to combine the problems of load tracking (of a previously committed load) and prediction (to define a future day-ahead load commitment) as penalties can be avoided simply by shifting production between the two days and changing the forecasted day-ahead consumption. To highlight how much flexibility can be gained by such an approach, Case 3 will be run neglecting the intraday market. Such a comparison is desirable for a couple of reasons. Firstly, the intraday market is much smaller than the day-ahead market and therefore it may not be possible to make large load adjustments. Thus, flexibility may need to be provided in other ways. Secondly, this should provide a best estimate of the load commitment in the second day. That being said, once again, this is a worst-case type scenario, as in practice it is possible to make

**Table 1**

Summary of the features considered in each of the different cases.

Case	Model Equations	Assumptions	Remarks
1	1–6, 7, 10, 15, 18–20, 23–24, 25, 27, 28, 29	No selling on intraday market: $\sigma_t = 0 \quad \forall t \in T$	Overly pessimistic state-of-the-art Solved as two subproblems each with a 24 h horizon Max consumption peak not penalized
2	1–6, 7, 10, 15, 18–20, 23–24, 25, 27, 28, 29	Committed load treated as a decision variable: $y_{t \in T_{hr}}^{CL}$ is a positive continuous variable and not a parameter	Overly optimistic state-of-the-art Solved as two subproblems each with a 24 h horizon Max consumption peak not penalized
3	1–29	No selling on intraday market: $\sigma_t = 0 \quad \forall t \in T$	More realistic approach Solved as one problem with a 54 h horizon Highlights flexibility gained from considering longer horizon Overall peak penalized
4–6	2–4, 6, 11–24, 27–34	No selling on intraday market: $\sigma_t = 0 \quad \forall t \in T$	More realistic approach Solved as one problem with a 54 h horizon Highlights flexibility gained from considering longer horizon Solved using proposed rolling horizon algorithm Detailed and aggregate peaks penalized instead of overall peak

some changes to the current committed load on the intraday market. However, we will show that it is still possible for this formulation to avoid many deviation penalties simply by shifting production in the aforementioned manner. A summary table of the different equations considered in each case, as well as some summary notes on each of these cases is presented in Table 1. Note that Cases 4–6 use the proposed rolling horizon approach and will be addressed in Section 4.2.

Case 1 and Case 2 were run for a daily production of 12 and 17 heats (denoted Case # - 12H and Case # - 17H) as two separate sub-problems (SP1/SP2), one for each of the two days considered. Case 3 was run with a time horizon of 54 h (two days plus six hours) with the total two-day production (24 and 34 heats) plus two additional heats (bringing the total to 26 and 36 heats) to account for production on the third day. The additional heats are necessary to illustrate that the production should be run continuously and not be interrupted towards the end of the day by allowing a heat to start at the end of the second day and finish in the next. To facilitate a fair comparison, a minimum production rate was set for each day, with the remainder of the heats being allowed to exit the continuous caster on the third day. Cases 1–3 were limited to 10,000 CPU seconds per problem/sub-problem. The reason for this was to give the optimizer enough time to find a reasonable solution, but to highlight the fact that such models are computationally too expensive to be used in an online setting.

A summary of the results of the tests can be seen in Table 2 with the resulting load profiles for some of the cases presented in Fig. 12. A few remarks about the presentation of the results follow. The first is that a direct comparison between the objective functions of Cases 1–2 and Case 3 is not possible. This is because different problems are being solved for each of these groups of cases. That being said, it is possible to compare key performance indicators regarding the amount of deviations paid, the max peak, and the load profile.

When looking at the results for Cases 1 and 2 it is clear that they are two extremes of the same problem. Case 1 is overly constrained, leading to substantially more deviations being paid, and therefore a much higher objective function. Conversely, Case 2 has too much freedom and reports an unrealistically low deviation

**Table 2**

Comparison of the results between the two one-day formulations and the novel full-space formulation.

Case	Deviations Paid (EUR)	Max Peak (MW)	CPU Time (s)	Objective Value	Gap (%)
1 - 12H	196,600	96	10,000 6893	358,147 337,552	<0.1/0
2 - 12H	120	177	10,000 3505	214,094 215,321	0/0.3
3 - 12H	25,100	94	10,000	1,074,763	8.6
1 - 17H	305,400	185	265 10,000	503,070 497,451	0/0.1
2 - 17H	7200	192	10,000 10,000	345,542 327,312	2.6/1.3
3 - 17H	16,500	177	10,000	1,663,405	19.3

amount. Comparing the integrated full-space two day problem (Case 3) to the two separate one day problems (Cases 1 and 2) clearly indicates that the novel formulation is able to avoid deviation penalties simply by transferring production across the current/next day boundary. This provides two main benefits, the first is that fewer deviation penalties must be paid by better tracking the committed load in day one. The second benefit is that the future day demand can be modified such that fewer deviations need to be paid in the future, and that the production plan can be adjusted to produce at time periods where electricity is cheaper. In the 12-heat case production was pushed forward from the second day to the first to avoid paying negative deviation penalties. Conversely, in the 17-heat case it is more favourable to slow down production to avoid paying positive deviation penalties. As expected from the definition of the cases, Case 3 has an intermediate value for deviations paid compared to Cases 1 and 2. This is because of the more realistic electricity market modeling in this case, and the unrealistic modeling of markets in Cases 1 and 2.

It is also evident that the new formulation is able to effectively manage the maximum peak within the confines of the production regime. In the 12-heat version of Case 2 the optimizer has complete control over the load profile. As a result, both EAFs were operated at the same time in order to shift production to cheaper times. When the peak is penalized in the two-day approach (Case

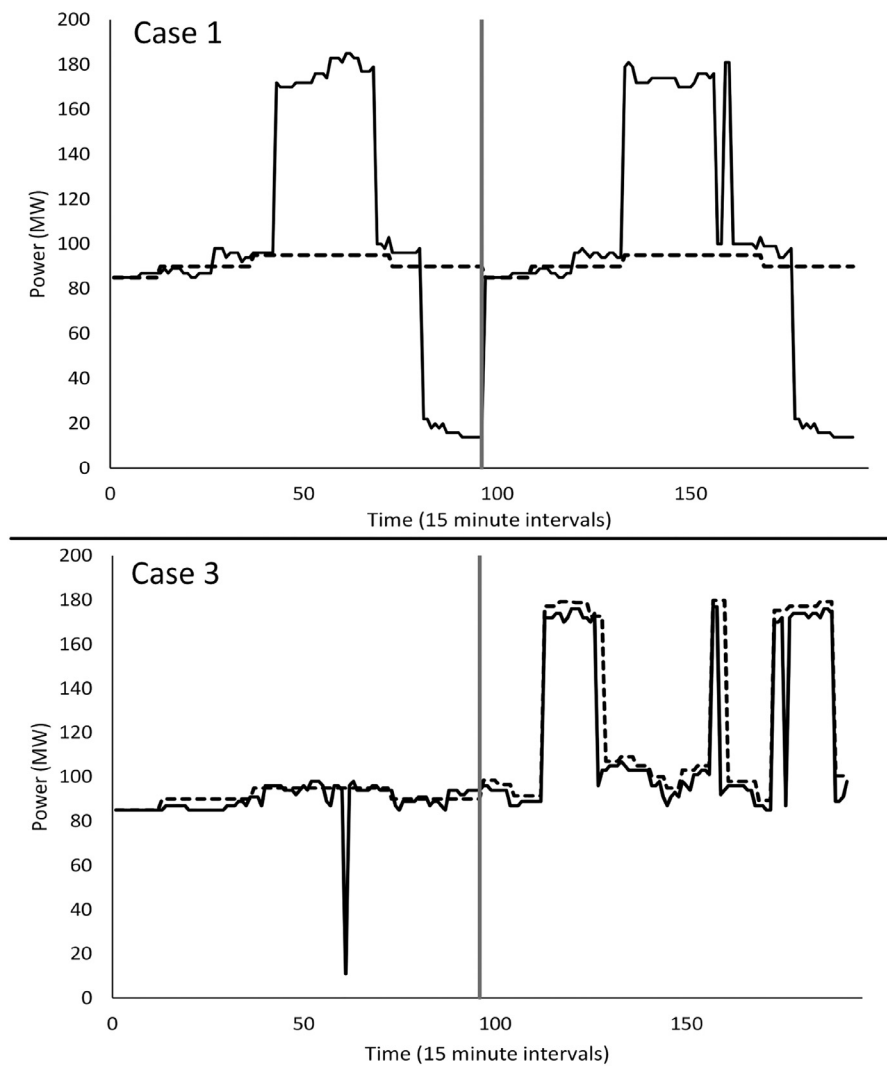


**Fig. 12.** Contracted (dashed line) and actual (solid line) electricity load profiles for the 17 heat trials of Cases 1 and 3. The gray line represents the division between Day 1 and 2 of the scheduling horizon.

3) only one EAF was used at a time, even though the formulation has the flexibility to define the load to be followed in the second day. This contrasts Case 1, which also only turns on one EAF at a time, not for the purpose of avoiding the peak, but in order to avoid paying deviation penalties. In the 17-heat case, peak management was more constrained due to the higher production amount, however, a smaller peak was still achieved by Case 3 than in both Case 1 and 2. These results indicate that it is necessary to consider the electricity peak in DSM situations.

The proposed two-day formulation in general has difficulties closing the optimality gap. The full-space models achieved at best a gap of approximately 9%. This is potentially due to many factors. One factor is the high dependency of all variables on time, as this problem considers hourly prices, hourly deviation prices, as well as a time-dependent penalty free regions. Another issue is due to the poor relaxation of the max-peak constraint. That being said, the formulation is still able to find solutions, within the constraints of the electricity markets, that exhibit the expected behaviour, and that provide more flexibility than the current standard of considering two single-day problems.

The two-day formulation, also rectifies the problem of production dropping off towards the end of the day as can be seen in Fig. 12. This represents a more realistic production scenario as each stage in the plant is operated continuously as opposed to operat-

ing the first stages only until the daily production has been met. This can be seen for both the full-space and the rolling horizon approaches. In all of the two-day cases the EAF is operated across the boundary between day one and day two, as well as between day two and day three. This contrasts the two one-day approaches which exhibits a characteristic spike in production in the middle of the day followed by a drop in electricity consumption for a few hours towards the end of the day. This unrealistic pattern can be seen in many previous DSM works (Castro et al., 2013), (Nolde and Morari, 2010), (Hadera et al., 2015). This is due to the short length of the scheduling horizon and the lack of integration between the two markets. In the middle of the day production must be rushed to ensure that targets can be met. Towards the end of the day, the considered jobs have all passed through the EAFs, thus there is a large drop in electricity consumption. While it is true that this peak-valley pattern is the result of an optimization problem, and appears to be cyclic, it should be stressed that this result only comes about due to the short length of the scheduling horizon and the associated market assumptions needed when considering such horizons. Therefore, it is not a truly cyclic production pattern. This is due to two main reasons. The first is that production orders, and their grouping, change on a day-to-day basis resulting in different production patterns. In this case, we look at two identical days of production resulting in similar patterns between the two days.



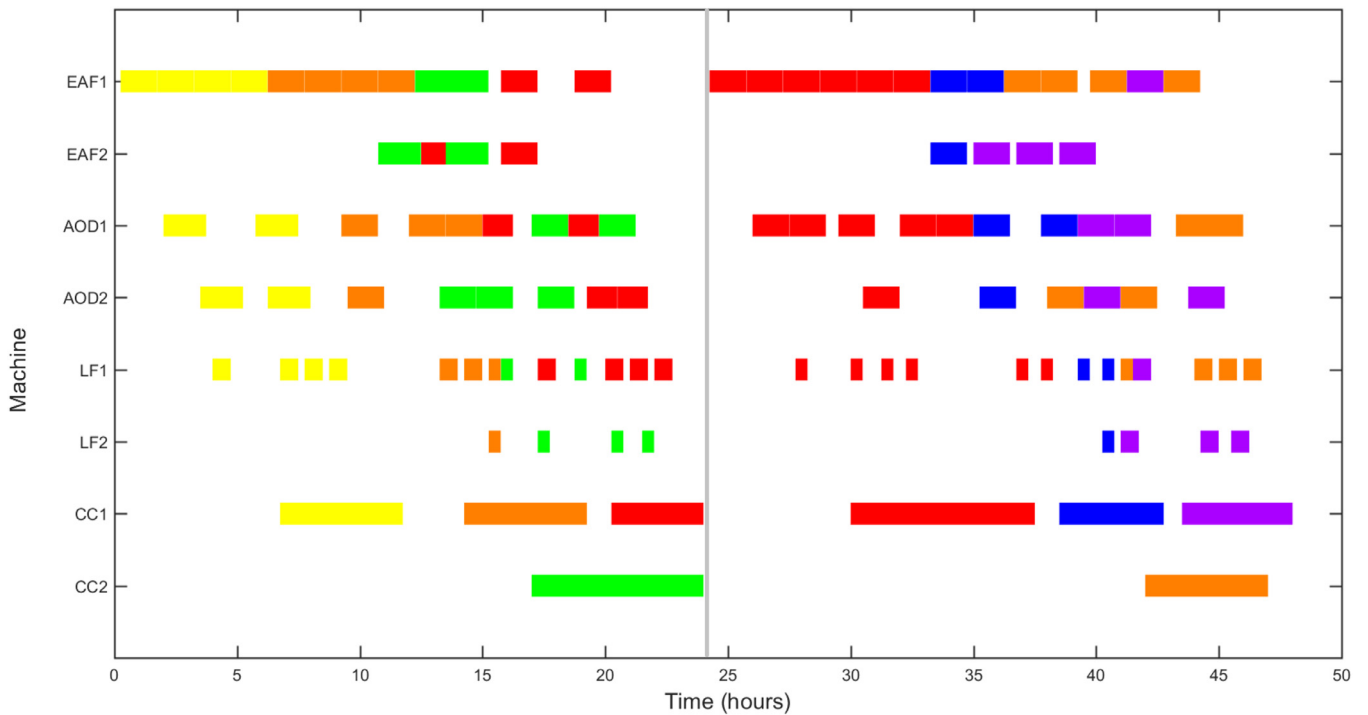


**Fig. 13.** Gantt chart for Case 1, solved as two separate one-day subproblems. Each color represents a different heat group and the gray line represents the division between Day 1 and 2 of the scheduling horizon.

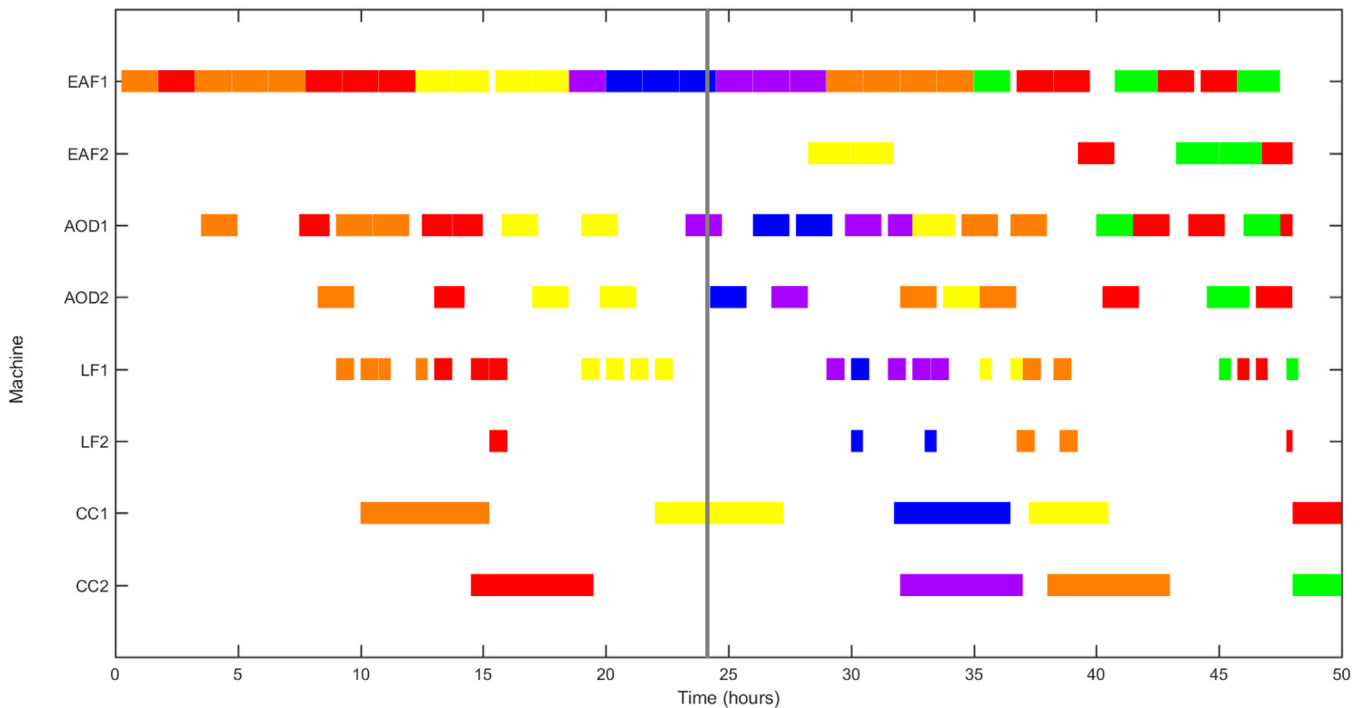


**Fig. 14.** Gantt chart for Case 4, solved as one two-day problem. Each color represents a different heat group and the gray line represents the division between Day 1 and 2 of the scheduling horizon.

This same type of analysis also extends to the electricity pricing scheme. Since electricity prices are dynamic, depending on the nature of these prices a true cyclic pattern will not be reached in practice. Another way of looking at this, from a practical point of view, is that the goal should be to maximize throughput, thus, it is undesirable to have large gaps in production between the two days. Furthermore, this prevents the ability to fully take advantage of time-based electricity prices as tasks are more constrained than they need to be. The two-day formulation does experience periods

of time where both of the furnaces are off however this is due to other factors. In any case, the novel formulation provides the opportunity for heats to start in one day and finish in the next, which can be seen in Fig. 14 where heat groups or even single operations are able to start in one day and finish in the next. This in turn allows one of the EAFs to be operated almost continuously over the entire duration of the scheduling horizon, which is not possible when considering only a single-day problem (as in Fig. 13). The same pattern can be seen among all the stages when considering

two single-day problems, which results in a clear separation between the two days of production.

#### 4.2. Comparison of full-space model and non-uniform grid approach

The goal of the non-uniform grid approach is to address the computational complexity that the results from the full-space two-day model. Therefore, three additional cases are defined to test the efficacy of the rolling horizon non-uniform grid approach. These cases, denoted Case 4, 5, and 6 are outlined as follows: Case 4, 5, and 6 use the same parameters as Case 3 but are calculated using the rolling horizon non-uniform grid approach. They are each run with a detailed period of 12 h, fixing the decisions for the first six hours and then extending the duration of the detailed model. To lessen the effects of the rounding errors due to the larger time slots in the aggregate model, the processing time of the unit is combined with the minimum transfer time ( $\tau_{i_{h,u},t}$ ; see Eq. (35)). The transfer tasks are then assigned a duration of zero time slots (i.e. the transfer tasks consumes the outlet location resource and produces the inlet location resource in the same slot;  $\tau_{i_{h,u},u',t} = 0$ ). The exact timing of the transfers is then sorted out in the detailed portion of the model. Cases 4–6 differ with respect to the subproblem solution times in the rolling horizon algorithm. Case 4

was limited to 600s per subproblem as 10 min is seen as an acceptable amount of time to report a schedule (Harjunoski et al., 2014). Case 5 was limited to 3600s per subproblem in order to allow each rolling horizon iteration to find a near-optimal solution. This was done in order to gather insights into the loss of optimality directly cause by the non-uniform grid approach. Case 6 was run until an optimality gap of 5% was achieved for each subproblem of the rolling-horizon approach. This is done to highlight the fact that reasonable solutions are found quickly, but significant computational effort is needed to find the true optimal solution as well as to close the optimality gap. A summary table of the different equations considered in each case, as well as some summary notes on each of the cases is, once again, presented in Table 1.

$$\tau_{i_{h,u},t} = \tau_{i_{h,u},t} + \tau_{i_{h,u},u',t} \quad \forall t \in T_{agg}, h \in H, k \neq 4, u \in U_k, u' \in U_{k+1} \quad (35)$$

A numerical comparison of the tests can be shown in Table 3 with load profiles for some of the cases shown in Fig. 15. When comparing the rolling horizon solutions to the full-space solution, the optimality gap is calculated relative to the best full-space solution. This is done for two reasons: 1) due to the heuristic nature of the rolling horizon algorithm, a true lower bound for the problem is not calculated. 2) this method provides an easy met-

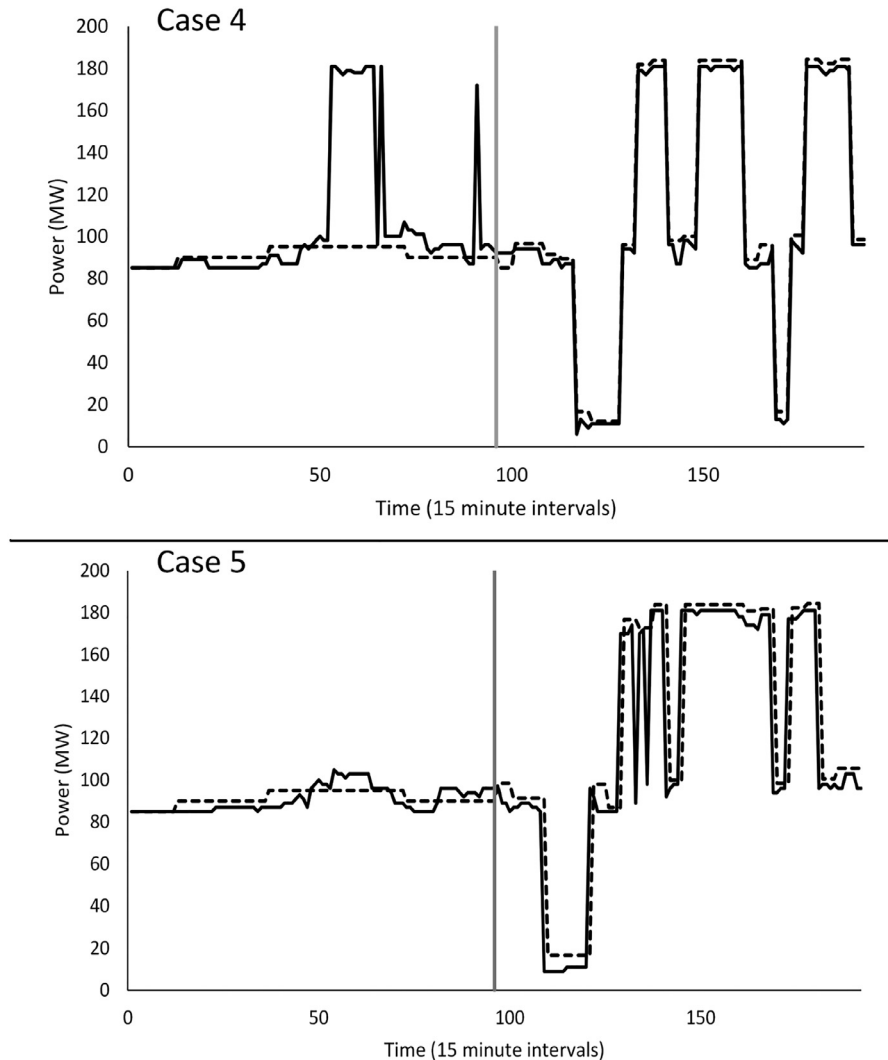


**Fig. 15.** Contracted (dashed line) and actual (solid line) electricity load profiles for the 17 heat trials of Cases 4 and 5. The gray line represents the division between Day 1 and 2 of the scheduling horizon.

**Table 3**

Comparison of the results between the novel full-space formulation and the proposed rolling horizon non-uniform time grid algorithm.

Case	Deviations Paid (EUR)	Max Peak (MW)	CPU Time (s)	Objective Value	Gap (%)
3 - 12H	25,100	94	10,000	1,074,763	0
4 - 12H - RH 600 s	37,400	96	3610	1,117,610	4.0
5 - 12H - RH 3600 s	6300	96	14,724	1,083,695	0.8
6 - 12H - RH 5% gap	55,388	101	507	1,148,933	6.9
3 - 17H	16,500	177	10,000	1,663,405	0
4 - 17H - RH 600 s	44,600	181	3456	1,730,301	4.0
5 - 17H - RH 3600 s	7150	181	21,638	1,695,366	1.9
6 - 17H - RH 5% gap	128,543	188	1480	1,872,902	12.6

ric to compare the quality of the rolling-horizon model to that of the full-space solution. The gap calculation equation can be seen in Eq. (36), where  $z$  is the objective function value of the case denoted in the subscript.

$$\frac{Z_{\text{non-uniform}} - Z_{\text{fullspace}}}{Z_{\text{fullspace}}} \quad (36)$$

The results also show that the non-uniform time grid approach, and the corresponding rolling-horizon scheme, are able to capture the key aspects of the formulation. For most cases, the rolling horizon scheme reaches a solution within a few percent of the full-

space solution. Case 5 was run with a maximum time limit of 3600 s for each sub-problem of the rolling horizon, and got to within a couple percent of optimality compared to the full-space model. This indicates that little optimality is sacrificed due to the aggregate nature of the non-uniform time grid approach. Comparing the two rolling horizon cases that terminate based on time (Cases 4 and 5), increasing the time limit per sub-problem of the rolling-horizon improves the solution quality by only a small percentage. Comparing the results from Case 6 to the results from Cases 4 and 5 it is possible to gain insight into the difficulty that the formulation has in converging to a provably optimal solution.

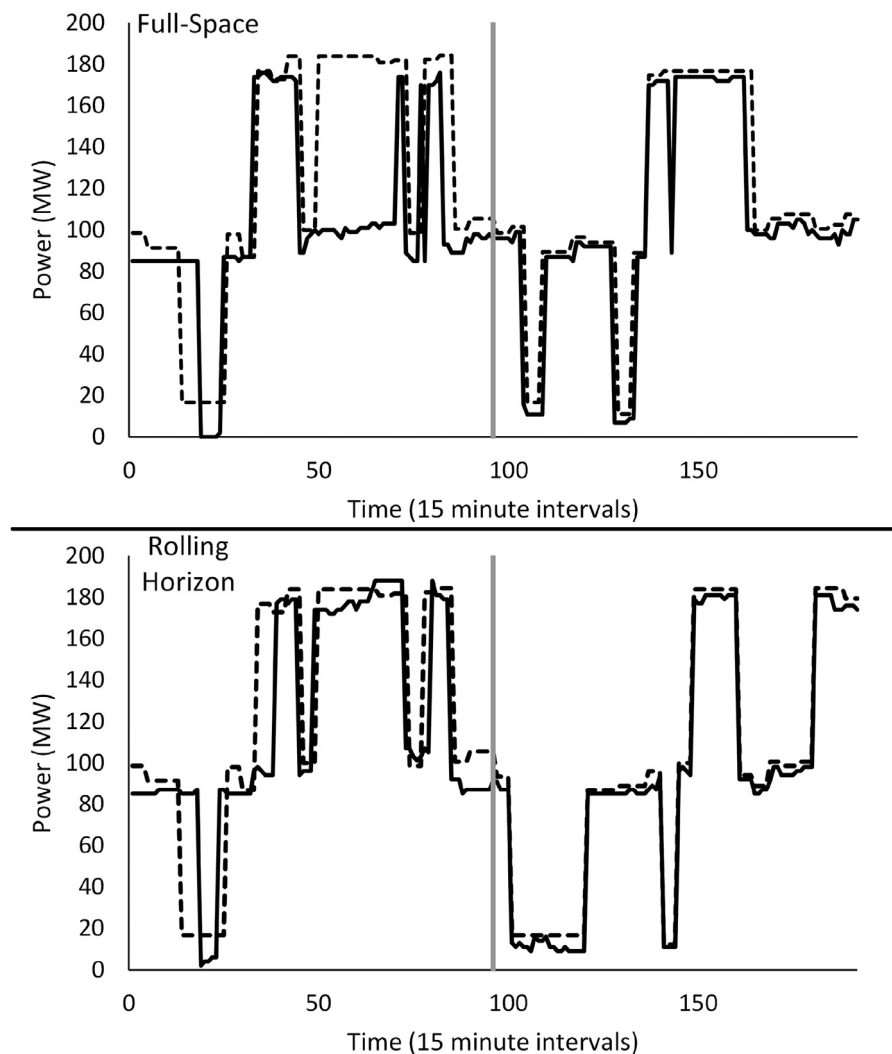


**Fig. 16.** Contracted (dashed line) and actual (solid line) electricity load profiles for the 17 heat cases load following case.

When limiting the optimality gap to 5% as is in Case 6, it can be seen that the computation time for the overall algorithm greatly decreases. This further indicates that the formulation is able to find near optimal solutions quickly, but has difficulty in closing the gap and proving optimality. The trade-off between computation time and solution quality is exemplified by Case 6, which, as expected, is worse than the solutions found for Cases 4 and 5. Taking all this into consideration, the rolling horizon algorithm settings for Case 4 (maximum 600 s per subproblem) will be used for subsequent tests of the algorithm as these settings were found to balance performance and solution quality well.

#### 4.3. Ability to follow the predicted load

This section investigates the ability of the proposed algorithm to follow the future load that it predicts. In this case, the predicted load is taken from the 17-heat scenario Case 5. This case was chosen as it was able to follow the previous given load in day one with minimal deviations and predicted an erratic load for the second day of the scheduling horizon. The scenarios here will use the predicted load from this case as their committed load for day one. The electricity cost profiles will also be switched between the two days to ensure that the same price profile that applied to the predicted load will now be used for the committed load. No initial

**Table 4**

Results from the predicted load following case. For the rolling horizon case the gap is calculated relative to the solution of the full-space model.

Case	Deviations Paid (€)	Max Peak (MW)	CPU Time (s)	Objective Value	Gap (%)
Full-space	121,400	176	10,000	1,789,887	17.1
Rolling Horizon	81,000	188	3025	1,803,129	0.7

solution will be given in order to rigorously test if the algorithm can correctly follow the load. In practice, it would be possible to seed an initial solution based on the output from the previous optimization that calculated the predicted load.

This case was run once using the full-space two-day model as well as using the non-uniform grid approach. A summary of the results can be seen in Table 4 and Fig. 16. From the results it is evident that the full-space model has difficulty dealing with the inconsistent predicted load. This is evident both in the large amount of deviations paid as well as the large optimality gap after 10,000 s. Once again, the formulation could not close the gap due to the high time-dependency of all the parameters. The effects of the optimality gap are far more evident in the load profile due to the highly fluctuating predicted load. It is interesting to note that the full-space formulation produced a very low peak, lower than

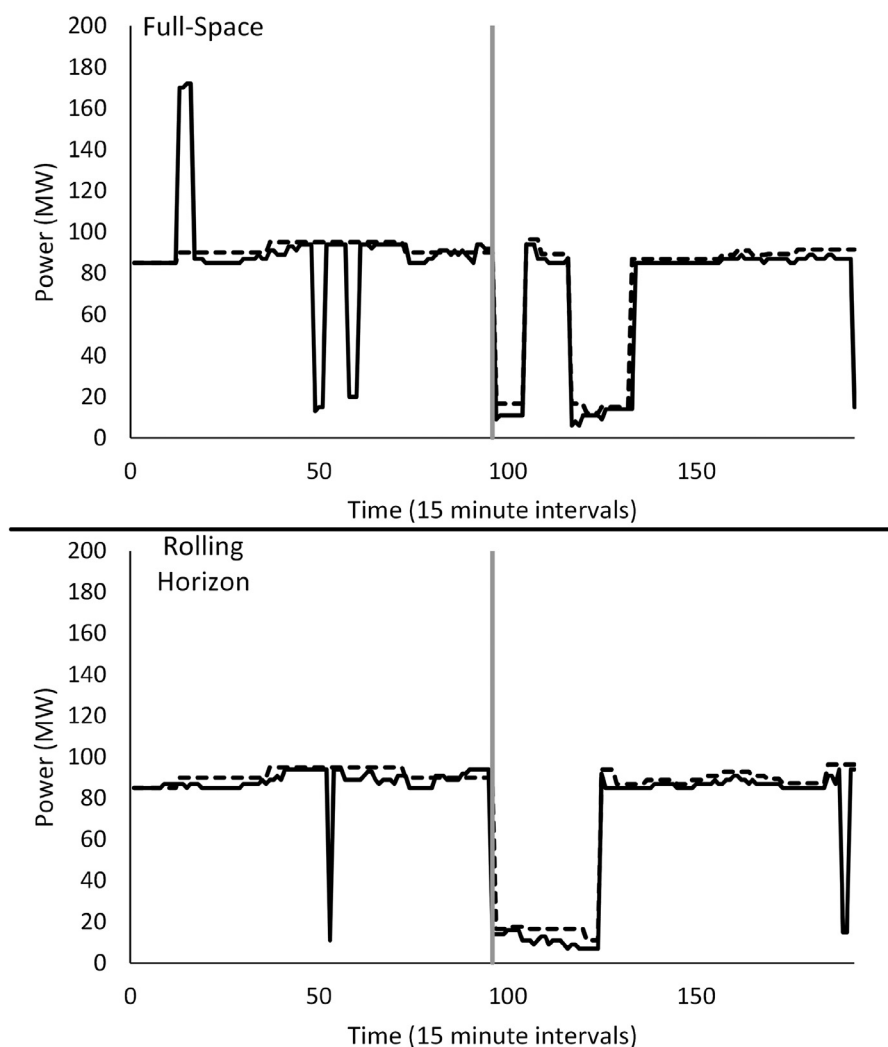


**Fig. 17.** Contracted (dashed line) and actual (solid line) electricity load profiles for the delayed heat test. The gray line represents the division between Day 1 and 2 of the scheduling horizon.



the 17-heat Case 3 in Section 4.1. Conversely, the rolling-horizon case was able to track the load much better than the full-space model paying only about two-thirds of the deviation penalties, resulting though, in a considerably higher peak load.

#### 4.4. Online tests/simulations

In order to test the ability of the non-uniform grid approach to respond quickly to disturbances, two case studies will be used. The first case will investigate a situation where an EAF will require an additional 60 min to process the current heat (Online Test 1). The second scenario will look at the addition of a rush order which needs to be completed by the end of day one (Online Test 2). The non-uniform grid approach for both cases will be updated with the information and rerun. Note that this is reasonable as a short term schedule will be provided after the first rolling-horizon iteration (limited to a computation time of 600 s) thereby quickly providing a plan to execute, while the remaining rolling horizon iterations will be used to determine the planning decisions (predicted load) as well as to schedule the whole horizon in detail. The full-space model will be updated by simply modifying the schedule determined by the full-space approach in Section 4.1 as it is too computationally expensive to be used in an online setting and did not re-

turn a solution to the given problems in 3600 s. This will be done by fixing the binaries from the earlier version of the schedule and allowing the new information to be optimally accounted for. For Online Test 1, this only allows for the updated timing for the longer batch as the full-space model is unable to return a solution with complete flexibility in the time constraints of one hour. For Online Test 2, the variables corresponding to the additional heats are unconstrained so they can be optimally inserted into the current schedule as once again the full-space model without the reduced binary space cannot find a solution in an hour.

The first case study utilizes the results from the 12-heat version of Case 3 introduced in Section 4.1. In this case, at the second hour mark of the horizon it is determined that the heat currently being processed in the EAF will require an additional 60 min. A table summarizing the results can be seen in Table 5 and the resulting load profiles can be seen in Fig. 17.

Results for this test indicate that the rolling-horizon scheme is able to respond to the disturbance by smoothing out the electricity consumption curve. The peak caused by the delayed EAF is clearly evident in the top graph (Full-Space) in Fig. 17 as the current schedule was simply updated to account for the delay. Conversely, in the bottom graph (Rolling Horizon) the subsequent heats were delayed to mitigate the effect of the disturbance. This

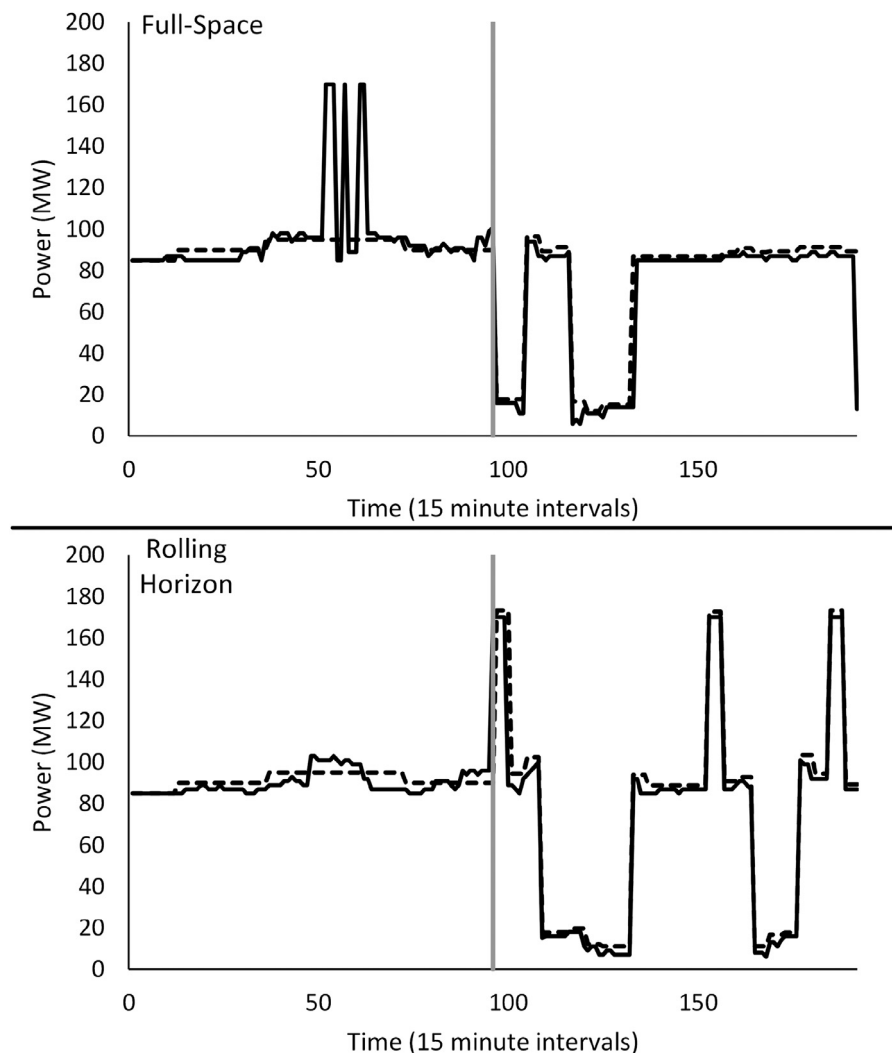
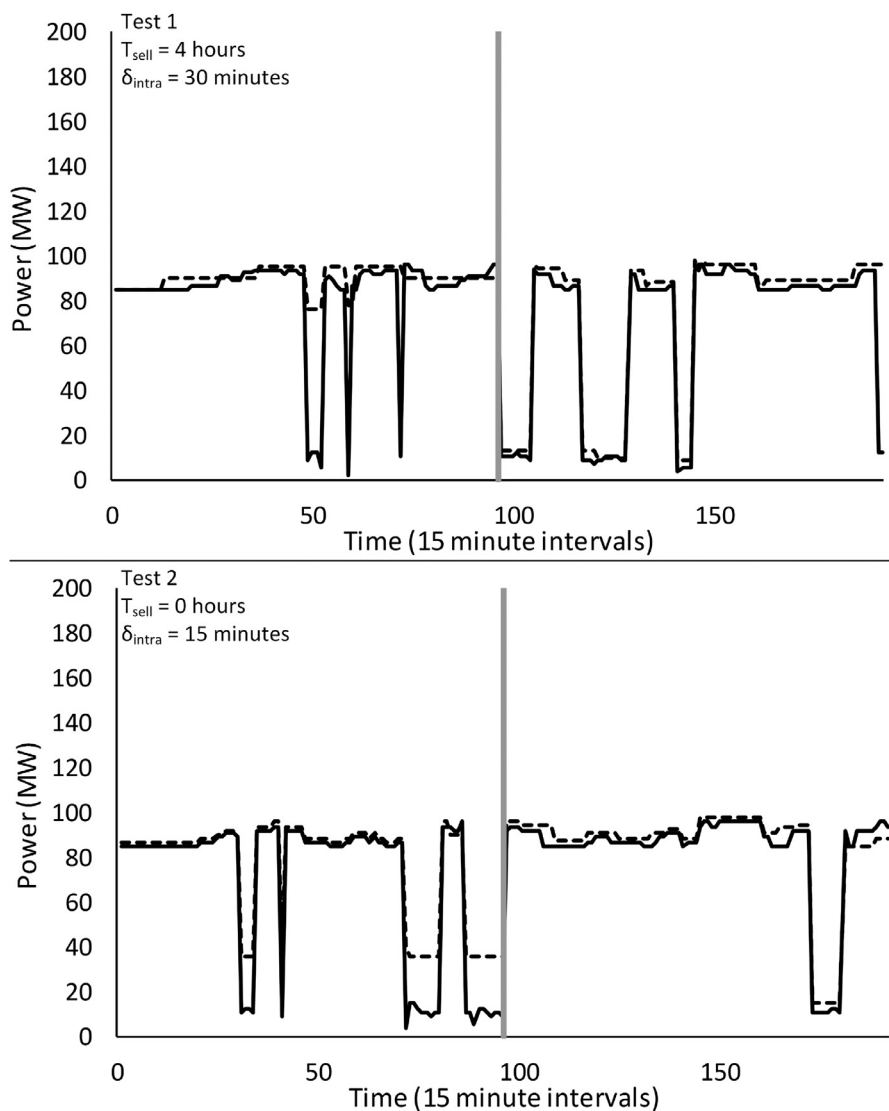


Fig. 18. Contracted (dashed line) and actual (solid line) electricity load profiles for the rush order test. The gray line represents the division between Day 1 and 2 of the scheduling horizon.



**Fig. 19.** Contracted (dashed line) and actual (solid line) electricity load profiles for the formulation flexibility tests. The gray line represents the division between Day 1 and 2 of the scheduling horizon.

**Table 5**  
Results from the delayed heat scenario.

Case	Deviations Paid (€)	Max Peak (MW)	CPU Time (s)
Full-space modification	47,550	172	< 5
Rolling Horizon	21,390	94	3098

has a double benefit. On the one hand, it prevents deviations from being paid, on the other it keeps the maximum peak to a level such that only one EAF is operated at a time.

Online Test 2 also utilizes results from the 12 heat version of Case 3 introduced in Section 4.1. In this case, a rush order of two heats (as part of their own group) is added during the first day to be finished by the end of the day. Once again, the full-space model will be updated to ensure that these heats are produced by the end of the day. This is accomplished by allowing the additional heats to be optimally inserted into the day one plan. The rolling-horizon approach will be run fixing the first hours of the schedule with the additional heats considered and constrained to be finished by the end of the first day. A table summarizing the results and the corresponding profiles can be seen in Table 6 and Fig. 18.

**Table 6**  
Results from the rush order simulation.

Case	Deviations Paid (€)	Max Peak (MW)	CPU Time (s)
Full-space	24,500	170	10,000
Rolling Horizon	13,500	170	3635

The results show that the non-uniform approach is able to effectively respond to the disturbance by shifting some of the non-essential heats from the first day to the second. This results in much fewer deviation penalties being incurred on the first day. Interesting in both cases a maximum peak of 170 MW was achieved. In the full-space approach this is unavoidable as the additional

heats must be produced by the end of the first day, thus both EAFs need to be operated at the same time. In the rolling-horizon approach, the maximum peak was achieved in the second day.

#### 4.5. Formulation flexibility

To show the flexibility of the multiple-time grid approach, two additional test cases follow. These cases are the same as the 26 version of Case 4 from Section 4.2, however, they include use of the intraday market. In the first test, it is possible to trade on the intraday market starting four hours into the horizon ( $T_{sell} = 4$  h), in interval sizes of 30 min. In order to account for the relatively smaller size of the intraday market, it is only possible to change the committed load by 10 MW in either direction. The second test is similar to the first one except it is possible to immediately trade on the intraday market in intervals of 15 min. In this case it is possible to change the committed load by 50 MW. Qualitative results from these cases are presented in Fig. 19.

The proposed formulation is able to handle the aforementioned tests simply by updating the model parameters to reflect the different electricity market situations. As can be seen from the graphs, when the intraday market and the discrete-time grid have the interval size ( $\delta = 15$  min) the committed load and the actual consumption match-up perfectly (except during periods of exceptionally large deviations). The objective functions for the two tests are € 742,023 and € 701,986 respectively. Intuitively, since test 2 has more flexibility, it is able to achieve a lower objective function value.

## 5. Conclusions

In this work a novel DSM scheduling formulation was proposed. The proposed formulation is based on the discrete-time RTN model (Pantelides, 1994) and applied to stainless steel making by expanding on the work of Castro et al. (2009). The novelty of the formulation stems from the fact that instead of considering an isolated one day problem, a two-day scheduling problem with different market constraints is solved. This allows for more realistic DSM modeling as it enables consideration of both the intraday and day-ahead markets in the same formulation. This in turn changes the DSM problem from one of just load following to a problem involving simultaneous load tracking and future load prediction. The formulation is further extended to consider grid operator fees based on the largest peak consumption of electricity.

The benefits of considering a two-day formulation are multifaceted. Firstly, this represents a more realistic modeling of electricity markets, which in-turn enables the possibility to avoid deviation from the total contracted load simply by shifting the production back-and-forth between the two days. Secondly, it allows production to start in one day and finish in the next one, producing more realistic electricity load profiles. Conversely, if only a one-day formulation is considered, there is a characteristic drop-off in production (and thus electricity consumption) towards the end of the day as the jobs considered in the scheduling model are completed. Additionally, the formulation is able to manage the maximum peak within the constraints of production.

The main drawback to the two-day formulation is that it results in large models that are computationally expensive and that have difficulties in converging to a provably optimal solution. To address this problem, a non-uniform time grid model was proposed. This model considers smaller time intervals towards the start of the scheduling horizon and longer aggregated intervals towards the end. This enables fast computation of a detailed schedule for the near future while ensuring feasibility over the entire horizon. To calculate the whole schedule in detail, the formulation can easily

be extended to a rolling-horizon scheme by fixing a subset of decisions in the current detailed interval and extending the length of the detailed interval. Results show that the non-uniform grid approach is able to capture the key aspects of the formulation in much smaller computational times than the full-space approach. Furthermore, the non-uniform grid approach was tested in various “online” simulation scenarios. The results show that the approach is able to respond to disturbances by recomputing a modified schedule for the near future, thus avoiding additional costs due to the disturbance.

This work extended modeling of markets in DSM formulations by considering both the intraday and day-ahead markets in the same optimization problem. That being said, there is still opportunity for more detailed modeling of market conditions that could further the applicability of DSM. For example, this work assumes that all bids on both markets are accepted at a given price for any quantity. Further work could investigate more accurate modeling of market bidding and clearing systems. Another drawback to the formulation is that the future predicted load can be erratic, making it difficult to track. Future work could investigate additional constraints to smooth predicted load profiles. Lastly, while the non-uniform grid approach can find good quality solutions quickly, there is still the potential for further speed-up algorithms, especially in regards to a rigorous decomposition approach that can preserve optimality.

## Acknowledgements

Financial support is gratefully acknowledged from the Marie Curie Horizon 2020 EID-ITN Project “PROcess NeTwork Optimization for efficient and sustainable operations of Europe's process industries taking machinery condition and process performance into account - PRONTO”, Grant agreement No. 675215.

## Appendix A. Model Notation

**Table A1**

Model notation. All variables are non-negative continuous unless otherwise specified.

Index/Set/Subset	
$r \in R$	Resources
$r \in R^{IL}$	Resources for steel heats at the inlet location of a stage
$r \in R^{OL}$	Resources for steel heats at the outlet location of a stage
$i \in I$	Tasks
$i \in I_{h,u}$	Processing task for heat $h$ that can be processed by unit $u$
$i \in I_{g,u}$	Processing task for heat group $g$ that can be processed by unit $u$
$i \in I_{h,u,u'}$	Transfer task for heat $h$ occurring between units $u$ and $u'$
$h \in H$	Steel heats
$g \in G$	Steel heat groups
$k \in K$	Processing stages
$u \in U$	Processing units
$u \in U_k$	Processing units at stage $k$
$t \in T$	Set of RTN time points
$t \in T_{detail}$	Set of RTN time points in the detailed portion of the non-uniform grid
$t \in T_{agg}$	Set of RTN time points in the aggregate portion of the non-uniform grid
$\theta$	Relative time to start of task
$t \in T_{hr}$	Set of hours in the time horizon
$t \in T_{peak}$	Set of times over which the peak is calculated
$t \in T_{intra}$	Set of times over which electricity is sold
$t \in T_{day1}$	Set of time slots that belong to the first day
<b>Parameters</b>	
$\tau_{i,t}$	Duration of task $i$ in time slots
$\delta$	Free variable - Time grid discretization for the uniform grid cases

(Continued)

**Table A1**  
(Continued)

$\delta_{T_{\text{detail}}}$	Time grid discretization for the detailed model
$\delta_{T_{\text{agg}}}$	Time grid discretization for the aggregate model
$\delta_{\text{intra}}$	Length of interval size for which it is possible to trade on the intraday market
$\mu_{r,i,t,\theta}$	Extend of discrete interaction of $r$ with $i$
$\max trf_{u,u'}$	Maximum transfer time between units $u$ and $u'$
$\min trf_{u,u'}$	Minimum transfer time between units $u$ and $u'$
$power_{h,u}$	Power consumption of heat $h$ in unit $u$
$T_{\text{sell}}$	Time until trading on the intraday market begins
$y^{BL}$	Amount of electricity load from a baseload contract
$\xi_{\text{toDate}}$	Largest peak achieved in this current billing period
$y_{\text{t}}^{\text{CL}}$	Total amount of current day committed electricity load
$y_{\text{t}}^{\text{TOU}}$	Amount of electricity load from a TOU contract
$y_{\text{t}}^{\text{BL}}$	Amount of electricity load from a baseload contract
$c_{\text{pf}}^{\text{DA}}$	Penalty free tolerance on load tracking
<b>Variables</b>	
$N_{i,t}$	Binary - execution of task $i$ at time slot $t$
$R_{t,t}$	Amount of $r$ available at $t$
$\Pi_{\text{rel},t}$	Electricity consumption at $t$
$\Pi_{\text{rel},t}^{\text{TOU}}$	Electricity consumption from the TOU contract at $t$
$\Pi_{\text{rel},t}^{\text{BL}}$	Electricity consumption from the BL contract at $t$
$\sigma_t$	Free variable - total amount of electricity load bought or sold on the intraday market
$\sigma_t^+$	Amount of electricity bought on the intraday market
$\sigma_t^{\text{DA}}$	Amount of electricity sold from the day-ahead contract on the intraday market
$\sigma_t^{\text{TOU}}$	Amount of electricity sold from the TOU contract on the intraday market
$\sigma_t^{\text{BL}}$	Amount of electricity sold from the base load contract on the intraday market
$y_t^{\text{PL}}$	Total amount of load to be purchased at time $t$ on the second day of the scheduling horizon
$y_t^{\text{DA}}$	Total amount of electricity the comes from the day-ahead market
$\Delta_t$	Total deviations from all the contract.
$\Delta_t^+, \Delta_t^{\text{DA}}$	Positive and negative deviations from the day-ahead committed load respectively
$\Delta_t^{\text{TOU}}$	Negative deviations from the TOU load
$\Delta_t^{\text{BL}}$	Negative deviations from the base load
$\xi$	Maximum electricity peak
$\xi_{\text{detail}}$	Maximum electricity peak in the detailed portion of the model
$\xi_{\text{agg}}$	Maximum electricity peak in the aggregate portion of the model
$\omega_t$	Free variable - penalty free zone from the day-ahead contract

**Table B2**  
Heats per group.

Group g	Heats	Consider in which problem sizes
1	H1-H4	12 and 17 heats
2	H5-H8	12 and 17 heats
3	H9-H12	12 and 17 heats
4	H13-H17	17 heats
5	H18-H21	12 and 17 heats
6	H22-H25	12 and 17 heats
7	H26-H29	12 and 17 heats
8	H30-H34	17 heats
9	H35-H36	Cases 3–6 12 and 17 heats

**Table B3**

Electricity price profile. Data was taken from the German Day-Ahead Market. (EPEx, 2017).

Hour	0	1	2	3	4	5	6	7
Price (€/MWh)	46.34	46.74	46.01	46.08	49.66	54.20	53.91	50.12
Hour	8	9	10	11	12	13	14	15
Price (€/MWh)	45.48	37.70	36.00	28.61	27.86	26.43	23.07	22.22
Hour	16	17	18	19	20	21	22	23
Price (€/MWh)	30.33	42.36	50.21	50.00	45.39	46.02	46.10	43.16
Hour	24	25	26	27	28	29	30	31
Price (€/MWh)	38.23	36.99	36.99	36.10	39.68	44.90	36.56	33.00
Hour	32	33	34	35	36	37	38	39
Price (€/MWh)	32.60	30.18	27.02	31.68	32.41	32.09	31.67	32.07
Hour	40	41	42	43	44	45	46	47
Price (€/MWh)	34.30	43.56	46.59	53.91	48.42	49.08	45.39	38.58

## References

- Ashok, S., 2006. Peak-load management in steel plants. *Appl. Energy* 83 (5), 413–424. doi:[10.1016/j.apenergy.2005.05.002](https://doi.org/10.1016/j.apenergy.2005.05.002).
- Basán, N.P., Grossmann, I.E., Gopalakrishnan, A., Lotero, I., Méndez, C.A., 2018. Novel MILP scheduling model for power-intensive processes under time-sensitive electricity prices. *Ind. Eng. Chem. Res.* 57 (5), 1581–1592. doi:[10.1021/acs.iecr.7b04435](https://doi.org/10.1021/acs.iecr.7b04435).
- Biondi, M., Sand, G., Harjunoski, I., 2017. Optimization of multipurpose process plant operations: a multi-time-scale maintenance and production scheduling approach. *Comput. Chem. Eng.* 99, 325–339. doi:[10.1016/j.compchemeng.2017.01.007](https://doi.org/10.1016/j.compchemeng.2017.01.007).
- Castro, P.M., Harjunoski, I., Grossmann, I.E., 2009. New continuous-time scheduling formulation for continuous plants under variable electricity cost. *Ind. Eng. Chem. Res.* 48 (14), 6701–6714. doi:[10.1021/ie900073k](https://doi.org/10.1021/ie900073k).
- Castro, P.M., Harjunoski, I., Grossmann, I.E., 2018. Expanding RTN discrete-time scheduling formulations to preemptive tasks. In: Eden, M.R., Ierapetritou, M.G., Towler, G.P. (Eds.), 13th International Symposium on Process Systems Engineering (PSE 2018). In: *Computer Aided Chemical Engineering*, Vol. 44. Elsevier, pp. 1225–1230. doi:[10.1016/B978-0-444-64241-7.50199-3](https://doi.org/10.1016/B978-0-444-64241-7.50199-3).
- Castro, P.M., Sun, L., Harjunoski, I., 2013. Resource-task network formulations for industrial demand side management of a steel plant. *Ind. Eng. Chem. Res.* 52 (36), 13046–13058. doi:[10.1021/ie401044q](https://doi.org/10.1021/ie401044q).
- Dalle Ave, G., Harjunoski, I., Engell, S., 2018. Industrial demand side management formulation for simultaneous electricity load commitment and future load prediction. In: Eden, M.R., Ierapetritou, M.G., Towler, G.P. (Eds.), 13th International Symposium on Process Systems Engineering (PSE 2018). In: *Computer Aided Chemical Engineering*, Vol. 44. Elsevier, pp. 1237–1242. doi:[10.1016/B978-0-444-64241-7.50201-9](https://doi.org/10.1016/B978-0-444-64241-7.50201-9).
- De Ridder, F., Claessens, B., 2014. A trading strategy for industrial CHPs on multiple power markets. *Int. Trans. Electr. Energy Syst.* 24 (5), 677–697. doi:[10.1002/etep.1725](https://doi.org/10.1002/etep.1725).
- EPEx, 2017. Market data day-ahead auction 23–24/10/17. [Online; accessed Oct 2017].
- Erbach, G., 2016. *Understanding Electricity Markets in the EU*. Technical Report. European Parliamentary Research Service.
- European Distribution System Operators for Smart Grids, 2015. *Adapting Distribution Network Tariffs to a Decentralized Energy Future*. Technical Report. European Distribution System Operators for Smart Grids.
- Fleten, S.-E., Kristoffersen, T.K., 2007. Stochastic programming for optimizing bidding strategies of a nordic hydropower producer. *Eur. J. Oper. Res.* 181 (2), 916–928. doi:[10.1016/j.ejor.2006.08.023](https://doi.org/10.1016/j.ejor.2006.08.023).
- Gupta, D., Maravelias, C.T., Wassick, J.M., 2016. From rescheduling to online scheduling. *Chem. Eng. Res. Des.* 116, 83–97. *Process Systems Engineering* - A

## Appendix B. Model Parameters

**Table B1**

Processing times for each of the heats at each of the stages.

Heat	EAF	AOD	LF	CC1	CC2
H1-H4	80	75	35	50	50
H5-H6	75	80	45	60	60
H7-H8	85	80	20	55	55
H9-H12	90	95	45	60	60
H13-H14	85	85	25	70	70
H15-H16	85	85	25	75	75
H17	80	85	25	75	75
H18	80	95	45	60	60
H19	80	95	45	70	70
H20	80	95	30	70	70
H21-H22	80	80	30	50	50
H23-H24	80	80	30	50	60
H25-H30	85	75	25	60	55
H31-H34	90	95	45	55	60
H35-H36	95	85	20	60	75



- Celebration in Professor Roger Sargent's 90th Year. doi: [10.1016/j.cherd.2016.10.035](https://doi.org/10.1016/j.cherd.2016.10.035).
- Hadera, H., Harjunoski, I., Sand, G., Grossmann, I.E., Engell, S., 2015. Optimization of steel production scheduling with complex time-sensitive electricity cost. *Comput. Chem. Eng.* 76, 117–136. doi:[10.1016/j.compchemeng.2015.02.004](https://doi.org/10.1016/j.compchemeng.2015.02.004).
- Harjunoski, I., 2016. Deploying scheduling solutions in an industrial environment. *Comput. Chem. Eng.* 91, 127–135. 12th International Symposium on Process Systems Engineering & 25th European Symposium of Computer Aided Process Engineering (PSE-2015/ESCAPE-25), 31 May – 4 June 2015, Copenhagen, Denmark. doi: [10.1016/j.compchemeng.2016.03.029](https://doi.org/10.1016/j.compchemeng.2016.03.029).
- Harjunoski, I., Grossmann, I.E., 2001. A decomposition approach for the scheduling of a steel plant production. *Comput. Chem. Eng.* 25 (11), 1647–1660. doi:[10.1016/S0098-1354\(01\)00729-3](https://doi.org/10.1016/S0098-1354(01)00729-3).
- Harjunoski, I., Maravelias, C.T., Bongers, P., Castro, P.M., Engell, S., Grossmann, I.E., Hooker, J., Méndez, C., Sand, G., Wassick, J., 2014. Scope for industrial applications of production scheduling models and solution methods. *Comput. Chem. Eng.* 62, 161–193.
- Henriques, M.V., Stikkelman, R.M., 2017. Assessing storage and substitution as power flexibility enablers in industrial processes. In: 2017 14th International Conference on the European Energy Market (EEM), pp. 1–6. doi:[10.1109/EEM.2017.7981916](https://doi.org/10.1109/EEM.2017.7981916).
- Leo, E., Engell, S., 2018a. Integrated day-ahead energy procurement and production scheduling. *Automatisierungstechnik* 66 (11), 950–963.
- Leo, E., Engell, S., 2018b. Multi-stage integrated electricity procurement and production scheduling. In: Eden, M.R., Ierapetritou, M.G., Towler, G.P. (Eds.), 13th International Symposium on Process Systems Engineering (PSE 2018). In: *Computer Aided Chemical Engineering*, Vol. 44. Elsevier, pp. 1291–1296.
- Méndez, C.A., Cerdá, J., Grossmann, I.E., Harjunoski, I., Fahl, M., 2006. State-of-the-art review of optimization methods for short-term scheduling of batch processes. *Comput. Chem. Eng.* 30 (6), 913–946. doi:[10.1016/j.compchemeng.2006.02.008](https://doi.org/10.1016/j.compchemeng.2006.02.008).
- Merkert, L., Harjunoski, I., Isaksson, A., Säynevirta, S., Saarela, A., Sand, G., 2015. Scheduling and energy - industrial challenges and opportunities. *Comput. Chem. Eng.* 72, 183–198. A Tribute to Ignacio E. Grossmann. doi: [10.1016/j.compchemeng.2014.05.024](https://doi.org/10.1016/j.compchemeng.2014.05.024).
- Nolde, K., Morari, M., 2010. Electrical load tracking scheduling of a steel plant. *Comput. Chem. Eng.* 34 (11), 1899–1903. doi:[10.1016/j.compchemeng.2010.01.011](https://doi.org/10.1016/j.compchemeng.2010.01.011).
- Pantelides, C., 1994. Unified frameworks for the optimal process planning and scheduling. In: *Proceedings of the Second Conference on Foundations of Computer Aided Operations*.
- Papadaskalopoulos, D., Moreira, R., Strbac, G., Pudjianto, D., Djapic, P., Teng, F., Papapetrou, M., 2018. Quantifying the potential economic benefits of flexible industrial demand in the european power system. *IEEE Trans. Ind. Inf.* 14 (11), 5123–5132. doi:[10.1109/TII.2018.2811734](https://doi.org/10.1109/TII.2018.2811734).
- Papageorgiou, L.G., Pantelides, C.C., 1996. Optimal campaign planning/scheduling of multipurpose batch/semicontinuous plants. 1. Mathematical formulation. *Ind. Eng. Chem. Res.* 35 (2), 488–509. doi:[10.1021/ie950081i](https://doi.org/10.1021/ie950081i).
- Paulus, M., Borggrefe, F., 2011. The potential of demand-side management in energy-intensive industries for electricity markets in germany. *Appl. Energy* 88 (2), 432–441. The 5th Dubrovnik Conference on Sustainable Development of Energy, Water and Environment Systems, held in Dubrovnik September/October 2009. doi:[10.1016/j.apenergy.2010.03.017](https://doi.org/10.1016/j.apenergy.2010.03.017).
- Shoreh, M.H., Siano, P., Shafie-khah, M., Loia, V., Catalão, J.P., 2016. A survey of industrial applications of demand response. *Electr. Power Syst. Res.* 141, 31–49. doi:[10.1016/j.epsr.2016.07.008](https://doi.org/10.1016/j.epsr.2016.07.008).
- Wassick, J.M., Ferrio, J., 2011. Extending the resource task network for industrial applications. *Comput. Chem. Eng.* 35 (10), 2124–2140. doi:[10.1016/j.compchemeng.2011.01.010](https://doi.org/10.1016/j.compchemeng.2011.01.010).
- Weron, R., 2014. Electricity price forecasting: a review of the state-of-the-art with a look into the future. *Int. J. Forecasting* 30 (4), 1030–1081. doi:[10.1016/j.ijforecast.2014.08.008](https://doi.org/10.1016/j.ijforecast.2014.08.008).
- Xu, W., Tang, L., Pistikopoulos, E.N., 2018. Modeling and solution for steelmaking scheduling with batching decisions and energy constraints. *Comput. Chem. Eng.* doi:[10.1016/j.compchemeng.2018.03.010](https://doi.org/10.1016/j.compchemeng.2018.03.010).
- Zhang, Q., Grossmann, I.E., 2016. *Planning and Scheduling for Industrial Demand Side Management: Advances and Challenges*. Springer International Publishing, Cham, pp. 383–414.
- Zhang, X., Hug, G., Harjunoski, I., 2017. Cost-effective scheduling of steel plants with flexible EAFs. *IEEE Trans. Smart Grid* 8 (1), 239–249. doi:[10.1109/TSG.2016.2575000](https://doi.org/10.1109/TSG.2016.2575000).
- Zhao, S., Grossmann, I.E., Tang, L., 2018. Integrated scheduling of rolling sector in steel production with consideration of energy consumption under time-of-use electricity prices. *Comput. Chem. Eng.* 111, 55–65. doi:[10.1016/j.compchemeng.2017.12.018](https://doi.org/10.1016/j.compchemeng.2017.12.018).